Development of a bi-polar impedance based sensor system and LabVIEW based software for analyzing analytes for probable applications in biomedical engineering.

A Thesis submitted in partial fulfilment of the Requirements for the degree of

Master of Technology

In

Biotechnology and Medical Engineering

Specialization: Biomedical Engineering

By

GAURAV DINESH KULKARNI

ROLL NO: - 213BM1006

Department of Biotechnology and Medical Engineering

National Institute Of Technology,

Rourkela

Odisha 769008

June 2015

Development of a bi-polar impedance based sensor system and LabVIEW based software for analyzing analytes for probable applications in biomedical engineering.

A Thesis submitted in partial fulfilment of the Requirements for the degree of

Master of Technology

In

Biotechnology and Medical Engineering

Specialization: Biomedical Engineering

By

GAURAV DINESH KULKARNI

ROLL NO: - 213BM1006

Under guidance of

Dr. Kunal Pal

Department of Biotechnology and Medical Engineering

National Institute Of Technology,

Rourkela

Odisha 769008

June 2015

DEPARTMENT OF BIOTECHNNOLOGY AND MEDICAL ENGINEERING
NATIONAL INSTITUTE OF TECHNOLOGY, ROURKELA
ODISHA, INDIA – 769008

CERTIFICATE

This is to certify that the thesis entitled "Development of a bi-polar impedance based sensor system and LabVIEW based software for analyzing analytes for probable applications in biomedical engineering." Submitted by Mr. Gaurav Dinesh Kulkarni bearing roll no. 213BM1006 in partial fulfillment of requirement for the award of Master of Technology in Biotechnology and Medical engineering with specialization in "Biomedical Engineering" during session 2013-15 at National Institute of Technology, Rourkela is an authentic work carried out by him under my supervision and guidance.

To best of my knowledge, the matter embodied in the thesis has not been submitted to any other University/Institute for the award of any other Degree/Diploma

Date: - 21 May, 2015

Place: - Rourkela

Dr. Kunal Pal

Dept. of Biotechnology and Medical engineering

National Institute Of Technology, Rourkela

ACKNOWLEDGEMENTS

First of all I would like to express my deep sense of respect and gratitude towards my guide Dr. Kunal Pal who is the guiding force behind my project work. I am indebted to him for his constant encouragement and advice in my academics. I consider myself very lucky to work with such a great mentor and great personality who has had a profound effect on my career and my outlook towards future.

Next, I want to thank all my lab-mates Uvanesh, Dibyajyoti, Suraj, Gauri Shankar and Haldhar sir for their support. My sincere thanks to PhD sir Mr. Biswajeet Champaty for his constant encouragements, help and suggestions. Also I would like to thank and appreciate for constant support of my best friends Gauresh, Kaustubh and Prathamesh who helped me to become a better person.

Finally I would like to thank my family for their sacrifice, love and support. They have been always my role model and will be forever. Thank you for your help to study, to work, to teach me how to live and to become a good person by heart.

Gaurav Dinesh Kulkarni

Roll No:-213BM1006

Dept. of Biotechnology and Medical engineering

National Institute Of Technology, Rourkela

Date: - 21 May, 2015

Place: - Rourkela

ABSTRACT

The application of Electrochemical Impedance Spectroscopy (EIS) in the field of biomedical engineering is not well known. In this research, an effort is being made to analyze electrical properties of saline solution. For this purpose aluminum thin film electrodes of different electrode spacing were fabricated. The electrical equivalent models were used to analyze the complex processes taking place at the electrode-electrolyte interface by varying the spacing and concentration of sample. The software for stability analysis was developed using LabVIEW. Most stable combinations of model and electrode were carefully selected using time and frequency domain parameters.

Table of Contents

List of Figures

Acronyms

PDMS	Polydimethylsiloxane
CPE	Constant phase element
EIS	Electrochemical impedance spectroscopy
DW	Distilled water
E40	Electrode system with 40 μm spacing
E80	Electrode system with 80 μm spacing
E150	Electrode system with 150 μm spacing
E300	Electrode system with 300 μm spacing
S1	Saline solution having 0.5 % strength
S2	Saline solution having 1 % strength
S3	Saline solution having 1.5 % strength
S4	Saline solution having 2 % strength
GH	Gelatin hydrogel
CS	Corn starch
BS	Boiled starch
SS	Soluble starch

1 Introduction and Objectives

1.1 Introduction

In this research, an effort is being made to design and evaluate the performance of a label-free impedance based electrochemical sensor. The sensor used is aluminium coating on glass slide. The advantage of aluminium layer is stability from oxidation reactions. The label-free operation reduces any extra cost required in the designing of the sensor. The transduction in the form of impedance is often used in many biological sample analyses. The sensor is designed in such a way that it contains variable electrode distances by keeping other dimensions constant. The distances are in the µm range as dimensions of most of the biological species including bacteria, protein, etc. falls in µm range. To use the liquid sample as an analyte, micropipette tips are cut. PDMS adhesive does the placement of tip over the sensor. The PDMS ensures proper fixation of the tips after heat drying for about 20 min.

The impedance converter circuit is used to acquire the impedance changes occurring at the sensor. The readings of the output voltage are noted for each frequency. The readings are taken for all the electrode systems. The frequency range used is 50 Hz to 10 kHz. It was observed that the output voltage was not stable after the frequency of 10 kHz. The impedance profiles are obtained for each electrode system using DW as sample. The DW is called control, and all the analysis is done using DW first.

To fit the impedance data, few models were selected. The models are (RQ)Q, (RQ)(RQ) and (RQ)(RQ)Re. The impedance profiles from each distance are fitted using all the three models. The method for curve fitting is a non-linear least square method. The squared differences between the observed values and mathematical values (from corresponding model) are used as parameter to fit and obtain the equivalent values. The ‘Q’ value is converted to equivalent ‘C’ using the formula for the CPE. This step is required as there is no Laplace equivalent for CPE.

The values obtained from the fitting are used as an input for the LabVIEW program. The LabVIEW has certain advantages like user-friendly interface and simplicity of the design. The program displays Bode plot, Nyquist plot and impulse response after accepting component values from the user. Bode plot gives the information about the location of the pole at crossover frequencies. Nyquist plot highlights some unique features about some

activation controlled processes. The impulse response evaluates the systems amplitude as time increases to an infinite value. The program also displays transfer function and pole-zero plot in Laplace domain. The stability can be determined by looking at the position of the poles. For the two systems with almost identical pole position, the stability can be determined either by impulse response or Nyquist plot.

The most stable electrode system is thus determined by the careful observation of all the parameters. This includes curve fitting coefficients and time constant. To select best-fit model, the model with higher correlation coefficients is considered. For the most stable distance, the electrode system with smallest value of the time constant is desired.

The combination of best model and stable electrode system is used for the further analysis of the saline solution of different strengths. Gel samples are also evaluated using the best model obtained from the analysis.

1.2 Objectives

1. To develop suitable hardware for the acquisition of impedance.
2. To design sensor for the analysis of EIS.
3. To develop software for EIS data representation.
4. Study impedance analysis using gel based sample.

2 Literature review

The importance of impedance is significant in the case of biological sample analysis. The electrochemical interface is highly complex, making the electrochemical reaction a very unpredictable process. Electrochemical Impedance Spectroscopy (EIS) is a powerful tool in the investigation of the dynamics of electrode double layer charges in the bulk or interfacial region across the sample-sensor interface [1]. The basics and fundamental theory of impedance are discussed below.

According to Ohm's law, resistance (R) is defined as the ratio of voltage (V) to current (I) and is a measure of opposition to the electric current through the conductor [1]. Apart from the usual resistance, there are two other mechanisms opposing the current flow in the electrical circuit: the inductance (L) and capacitance (C). The inductance and capacitance are together formed the reactance (X). For AC circuits, the resistance is called impedance (Z). The DC signal can be defined as AC signal at the frequency tending to zero. Unlike ideal resistance, which has only magnitude the impedance possesses both the magnitude and the phase angle. The unit of impedance is the same as that of resistance [1]. In the complex plane, the real part of impedance is resistance and the reactance forms the imaginary part of the impedance.

Sensors are said to be the devices, which mainly consists of an active sensing element with a signal transduction unit. These two primary components in sensors transmit the signal from a sample or a change in a reacting species during the chemical reaction [2]. These devices generate output in any one of the signals as electrical, thermal or optical signals that could be interpreted using appropriate instrumentation. Type of the output signal is one of the methods of classifying these sensors. Out of these, electrochemical sensors forms the significant role in the analysis of the biological sample. These consists of the sensing electrodes capable of sensing analytes without any change in its physical or chemical structure. The sensors are designed particularly for the detection of the analyte in solid, liquid or gas phase. The electrochemical sensors are classified broadly into potentiometric, amperometric and impedometric /conductometric subtypes [3].

In potentiometric sensors, the potential difference between the working electrode and reference electrode is used to determine the ionic concentration of the electrochemical species in the chemical reaction. Nernst equation gives the relationship between the potential and the concentration. For biological applications, these sensors make use of

ion-selective electrodes, which convert biological reaction into the electrical signal. The example of such transduction includes pH sensor [4].

Amperometric types of sensors measure current resulting from the oxidation or reduction reaction of a particular species in the chemical reaction. If the current is measured continuously by keeping the voltage constant, it is termed as amperometry. Similarly, if the variable quantity is current, the process is called as potentiometry. An example of amperometric sensor includes detection of glucose concentration in the blood. In the glucose measurement, the current produced is the result of the formation of hydrogen peroxide [5].

Impedometric and conductometric devices are related by the inverse relation between the conductance and the impedance. The change in conductivity of the solution over time is measured in this devices. By combining the results with EIS, we can get more detailed information about the electrode-electrolyte interface and sample under test.

The electrical impedance based sensor are found to give promising results in the situations where low cost, portability and speed of operations are desired. One of the possible areas of application is bedside diagnosis and monitoring [6]. Other applications include bacterial detection in water, conductivity monitoring, cell-culture studies, etc. [7]

Most of the electrochemical sensors especially biosensors requires a label attached to the target. In this case, the results are based on the amount of the label detected [8]. Some of the labels are active enzymes, fluorophores, magnetic beads, etc. This approach is called labeled detection. In label-free detection, the interaction of the target and sensor brings about the changes in the electrical properties of the surface. Thus, no label is required for sensing the impedance. The label-free operation saves time and cost of sample handling [9].

Electrochemical Impedance Spectroscopy (EIS) is a modern and powerful tool for analyzing the electrical properties of materials and their interfaces with electronically conducting electrodes. To evaluate the electrochemical behavior of electrode and electrolyte materials, electrical measurements are usually made with cells having a minimum of two electrodes. The standard approach is to apply an electrical stimulus (in the form of a known voltage or current) to the electrodes and observe the response (the resulting current or voltage) [10].

A large number of fundamental microscopic processes take place throughout the cell when it is stimulated electrically that lead to the overall electrical response [10]. Some of the common phenomenon include the transport of electrons through the conducting electrodes, the transfer of electric current at the electrode–electrolyte interfaces towards or away from charged or uncharged atomic species that originate from the cell materials and its atmospheric environment (chemical reactions).

For the analysis of electrochemical sensor, EIS analysis algorithm shown in fig. 1 can be used [10]. First excitation in the form of current or voltage is used, and output values are noted. We can obtain impedance profiles (impedance versus frequency) from the output values. Suitable electrical equivalent models are selected depending upon the nature of the electrochemical sensor and type of the analyte used. Curve fitting is performed on the EIS data of the impedance profile obtained experimentally and its mathematical equivalent model. The result of this fitting will be the electrical values of the model. These values are useful for further analysis in either time or frequency domain analysis of the sensor system.

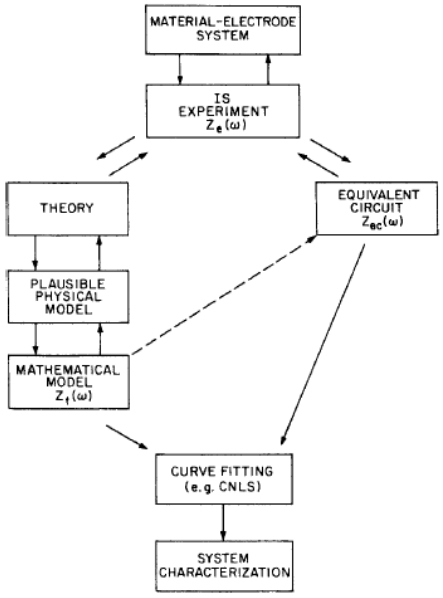

Fig. 1 EIS analysis algorithm

EIS data is commonly analyzed by fitting into an equivalent electrical circuit model [11]. Non-linear least square based fitting is one of the commonly used methods for curve fitting. Most of the circuit elements in the model are common electrical components such

as resistors, inductors, and capacitors. For an ideal resistance, the impedance will be purely real, and the current will always be in phase with the voltage across it. The impedance of an ideal inductor and capacitor will be purely imaginary. The impedance profile of an inductor will be opposite to that of a capacitor. An inductor's impedance is directly proportional to frequency, whereas the capacitor's impedance follows inverse relation with frequency.

EIS models usually consist of some electrical elements connected in the network either in series and/or parallel combinations. For the biological sample, it is very common to use CPE in the equivalent model [1]. The most commonly used models have been shown in following figure (fig.2)

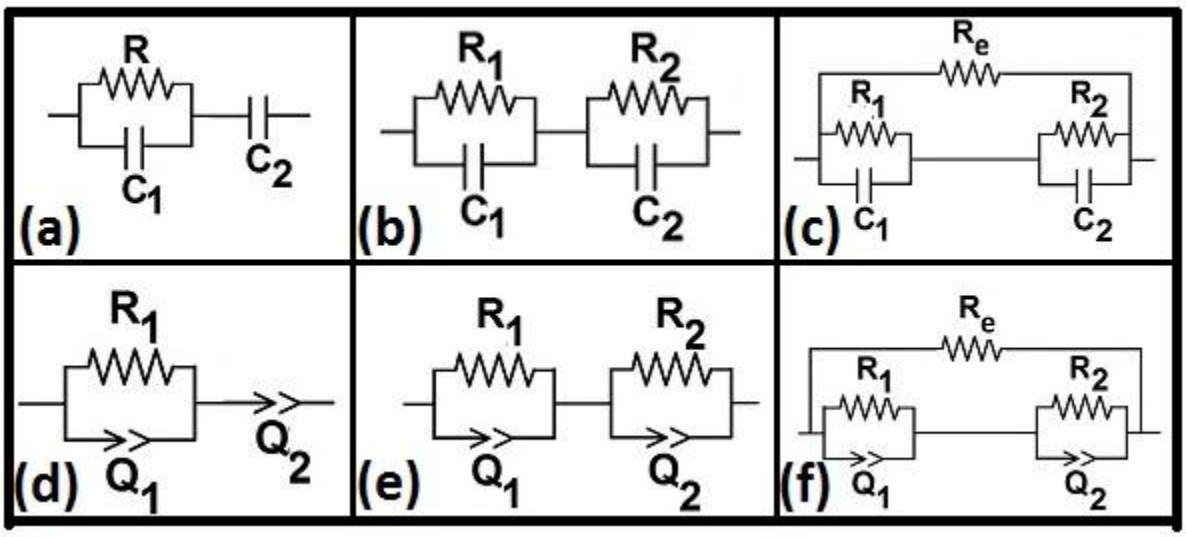

Fig. 2 Equivalent circuit models. (a) (RC)C, (b) (RC)(RC) (c) (RC)(RC)Re, (d) (RQ) Q, (e) (RQ)(RQ) and (f) (RQ)(RQ)Re

Nyquist plot, bode plot and impulse response are commonly used to represent EIS data. Nyquist plot is plotted between the real and imaginary components of the impedance. For Nyquist plot, real part ids plotted on x-axis while, the imaginary part is the y-axis. The impedance on the plot can be represented as the vector as shown in fig. 2, which shows

Nyquist plot for parallel RC circuit. High-frequency data is on right side of the plot, and low-frequency information is on right side. The shape of the semicircle mainly depends on the time constants present [12].

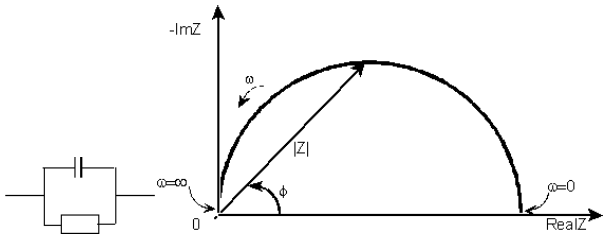

Fig. 3 Nyquist plot for typical parallel RC circuit

The Bode plot is a combination of magnitude and phase response of the system. In this plot, impedance is plotted against the log of frequency on x-axis both as an amplitude and phase shift on the y-axis. Bode plot gives explicit information about the frequency [1]. The nature of Bode plot mainly depends on the values of the circuit components. Fig. 3 shows Bode plot for parallel RC circuit.

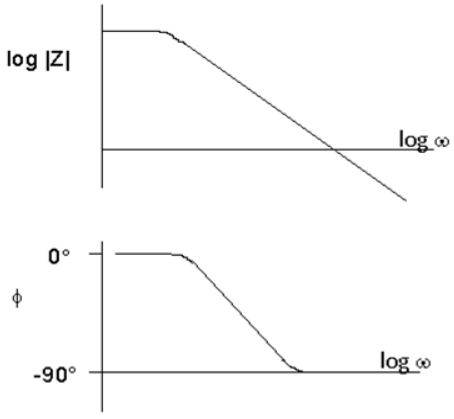

Fig.4 Bode plot for parallel RC circuit.

The impulse response is one of the test signals to evaluate the system's time response. Depending upon the order of the system, the nature of the impulse response changes. It is the plot of amplitude versus time. For any stable system, as time increases, the

amplitude should decay to zero value. This depends on the time constant, which in turn depends on the poles of the system. If the poles lie on right-hand side of the s-plane, the impulse response will be exponentially growing, and the system is said to be unstable.

Following parameters can be inferred from the EIS analysis.

1. Solution resistance: The resistance associated with the electrolyte.
2. Double layer capacitance: Electrical double layer exists at the electrode-electrolyte interface. This results in equivalent capacitance called double layer capacitance. The value of this capacitance depends on the electrochemical reactions, applied voltage, temperature, impurity, types of ions, ionic concentrations, etc.
3. Faradaic resistance: The resistance resulted from the charge transferred across the electrified interface as a consequence of an electrochemical reaction.
4. Activation controlled and diffusion controlled processes: In electrochemical reaction, the electrode potential determines the rate of reaction. This process depends on the arrival and supply of the electro-active species to the electrode. If the number of these species is more, the rate of reaction is determined by the electrode potential. This process is called as an activation controlled process. On the contrary, if the arrival of species is slow, the rate of reaction is controlled by passive processes like diffusion. This is called as diffusion control process. These two processes can be predicted from the nature of Nyquist plot. Bode plots do not give any information about these processes occurring for a particular electrode-electrolyte interface. On the positive side, Bode plot provides the information about frequency as the abscissa in this plot is frequency.

3 Materials and Methods

3.1 Materials

Copper clad board, glass slides, IC (OP-07, analog devices, US), resistances, connecting wires were procured from the local suppliers. Aluminum block (99.99 % pure) was purchased from, Function generator was purchased from dynalog, India. Digital storage oscilloscope was purchased from Techtronix. Lab VIEW 2010 (National Instruments, US), MS Excel 2013 (Microsoft, US) were used for the analysis. PDMS (Polydimethylsiloxane) and micro-tips were provided as a gift by Prof. Indranil Banerjee.

3.2 Methods

3.2.1 Fabrication of electrodes

Thin films of aluminum of thickness of 200 µm were deposited on microscopic glass slides by vacuum thermal evaporation technique as reported by *Amusan et. al.* The spacing between the electrodes was kept 40 µm, 80 µm, 150 µm and 300 µm. The electrodes were regarded as E40, E80, E150 and E300 respectively.

3.2.2 Determination of stability of the electrode by electrical modelling

Small wells were prepared by cutting the pieces of micropipette tips. The wells were fixed over the electrodes using PDMS substrate. 200 µl of the distilled water was put in the wells and the modulus of impedance at frequency range of 50 – 10 kHz was determined using in-house developed impedance analyzer. A sinusoidal wave was used for the analysis. The amplitude of the sinusoidal signal for the analysis was 1 $V_{(p-p)}$. The impedance data obtained were fitted to mathematical models representing (RQ)Q, (RQ)(RQ) and (RQ)(RQ)Re electrical models using solver add-in of Microsoft Excel 2010. The stability of the equivalent electrical circuit was predicted and the most stable model

was used for the analysis of saline solution of different strengths. A correlation coefficient amongst the experimental and the calculated values (from models) was determined to get the best fit model.

3.2.3 Hardware development

3.2.3.1 Multisim design

The circuit of the impedance converter is first designed in NI Multisim 2010 (purchased from National Instruments, US). This has been shown in fig.1. The circuit consists of three op-amp based impedance converter. All the op-amps were purchased from analog devices, US.

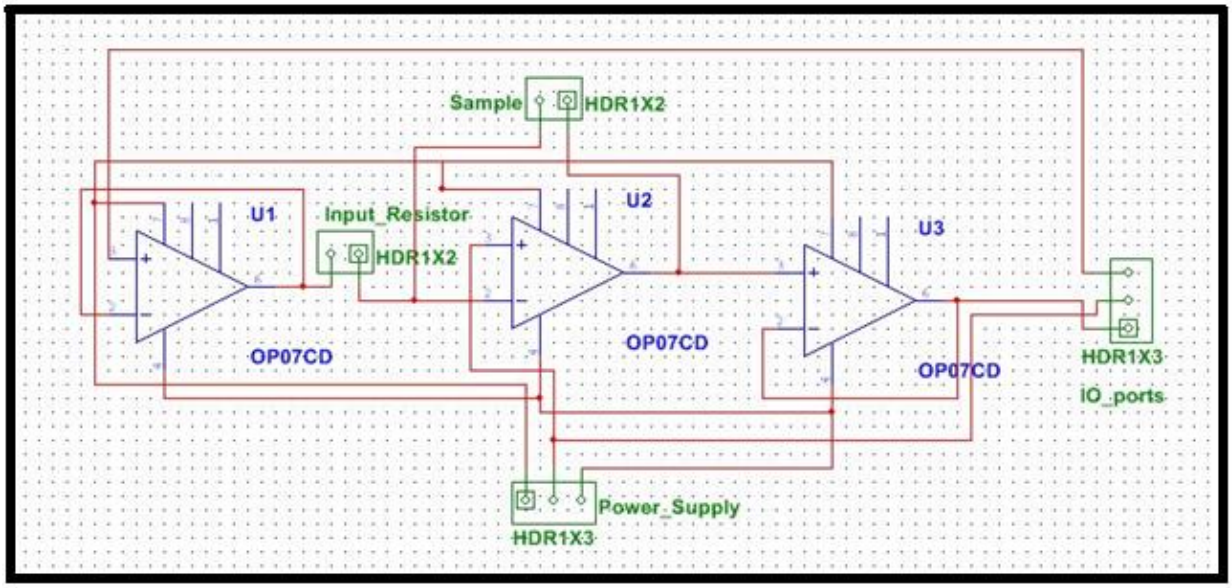

Fig. 5 Screenshot of Multisim design.

The op-amps U1 and U3 were used in voltage buffer configuration for impedance matching at input and output terminals respectively. The op-amp U2 was configured as inverting amplifier with sample placed in feedback loop. Three connectors were used in this design. For the connections of the sample, power supply and I/O terminals connectors (HDR 1x2, HDR 1x3 and HDR 1x3 respectively) were used. The 3D layout of the circuit design has been shown in fig. 2.

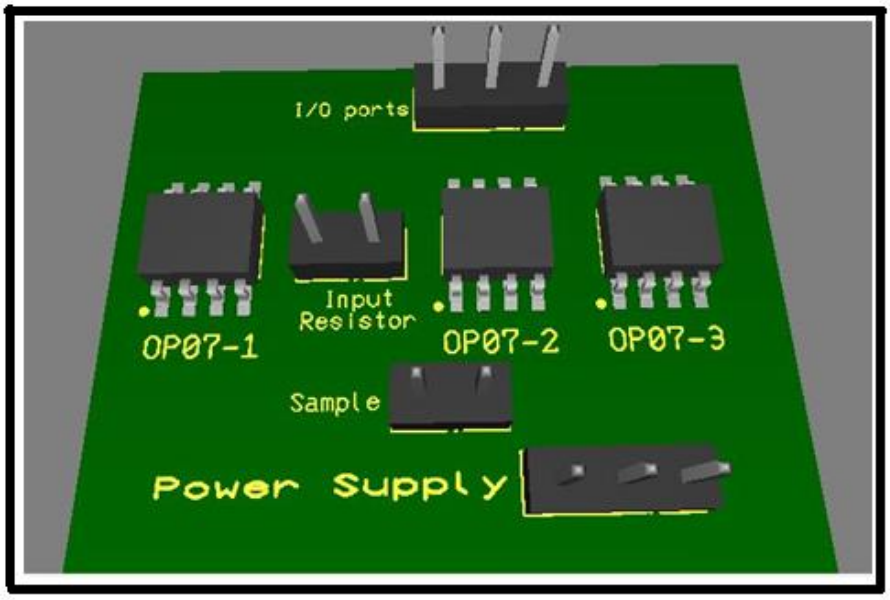

Fig. 6 Screenshot of 3D layout.

3.2.3.2 Ultiboard design

The Multisim design was transferred to Ultiboard (purchase from National Instruments, US). The screenshot of transferred design has been shown in fig. 3.

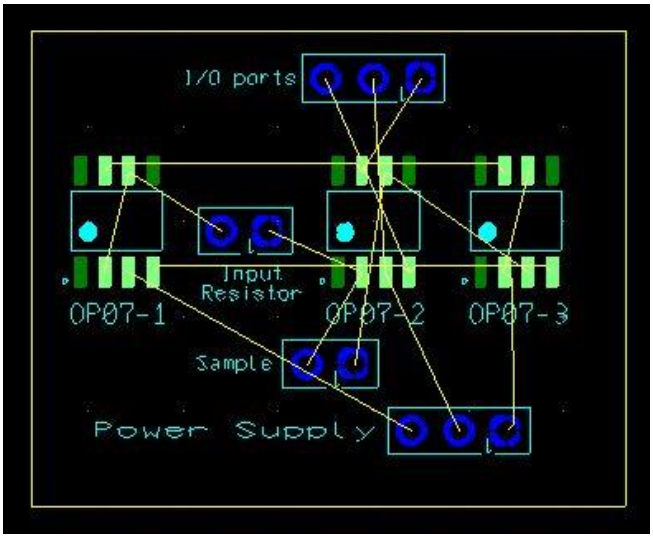

Fig. 7 Screenshot of design transferred to Ultiboard.

For the PCB layout, copper bottom layer of 1 mm thickness was selected. The pictograph of the hardware connection has been shown in fig. 4.

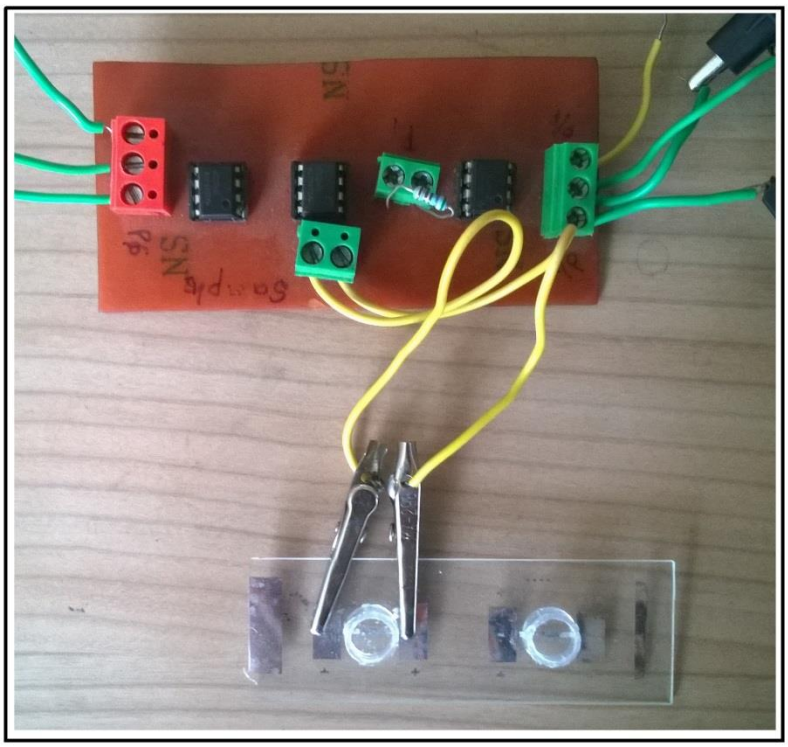

Fig. 8 pictograph of complete hardware with sensor connection.

3.2.4 Software development

The models (RQ)Q, (RQ)(RQ) and (RQ)(RQ)Re were analyzed using in-house developed LabVIEW program. The version of LabVIEW software used was 2010 (purchased from National Instruments, US). Multiple event structures were designed to calculate transfer function based on the model. The mouse-up event was assigned to perform the selection of model. After the event has been registered, the user dialogue box was prompted to accept the values from the user. The conversion of Q into equivalent C is necessary before entering the parameter values. The program accepts the user values and convert them into transfer function model as in equation 6. The transfer function is calculated in Laplace domain and script node was used for calculating the transfer function coefficients. After the calculation, transfer function, pole zero plot, bode plots, Nyquist plots and

impulse response were generated. The tab control was used to show all these parameters in tabular format. Picture ring was used to display the picture of the equivalent model when particular model was selected. The front panel also contains controls for the selection of starting frequency, ending frequency and number of points. For impulse response, the control for selecting start time, end time and the interval was created. The stability of the transfer function can also be displayed. The stop button control was also handled by event structure.

$$H(s) = \frac{b_0 + b_1 s + ... + b_m s^m}{a_0 + a_1 s + ... + a_n s^n} \qquad (1)$$

Fig. 9 shows the screenshot of complete front panel. Fig. 10 shows the screenshot of the program with user dialogue box. The screenshot of the block diagram of the event corresponding to (RQ)(RQ) model has been shown in fig. 11. The screenshots of representative graphs generated has been shown in fig. 12.

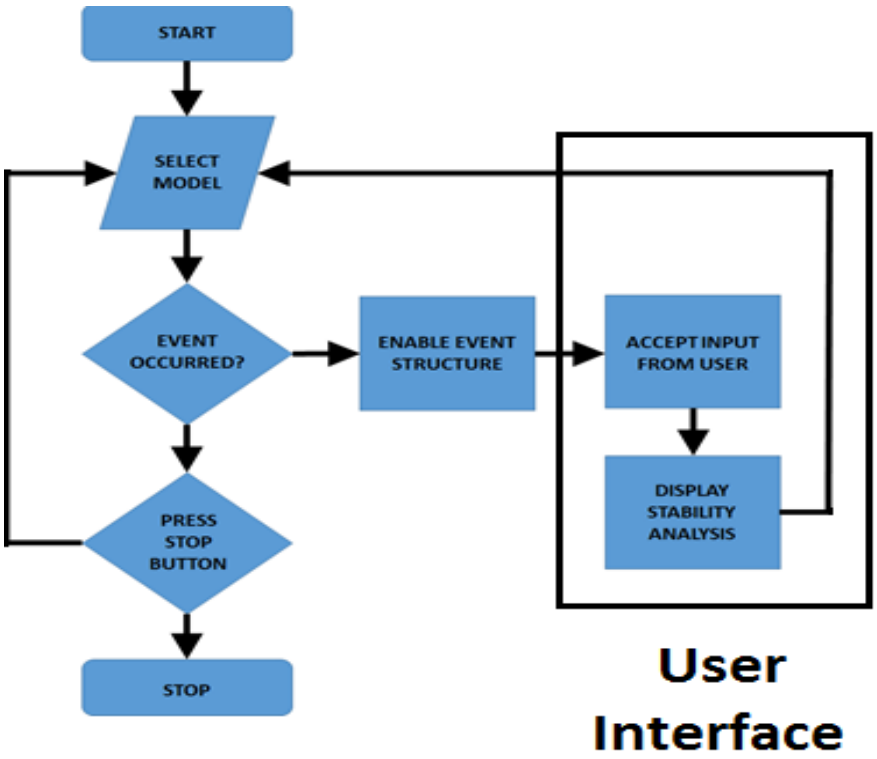

Figure. 9 Algorithm of LabVIEW program.

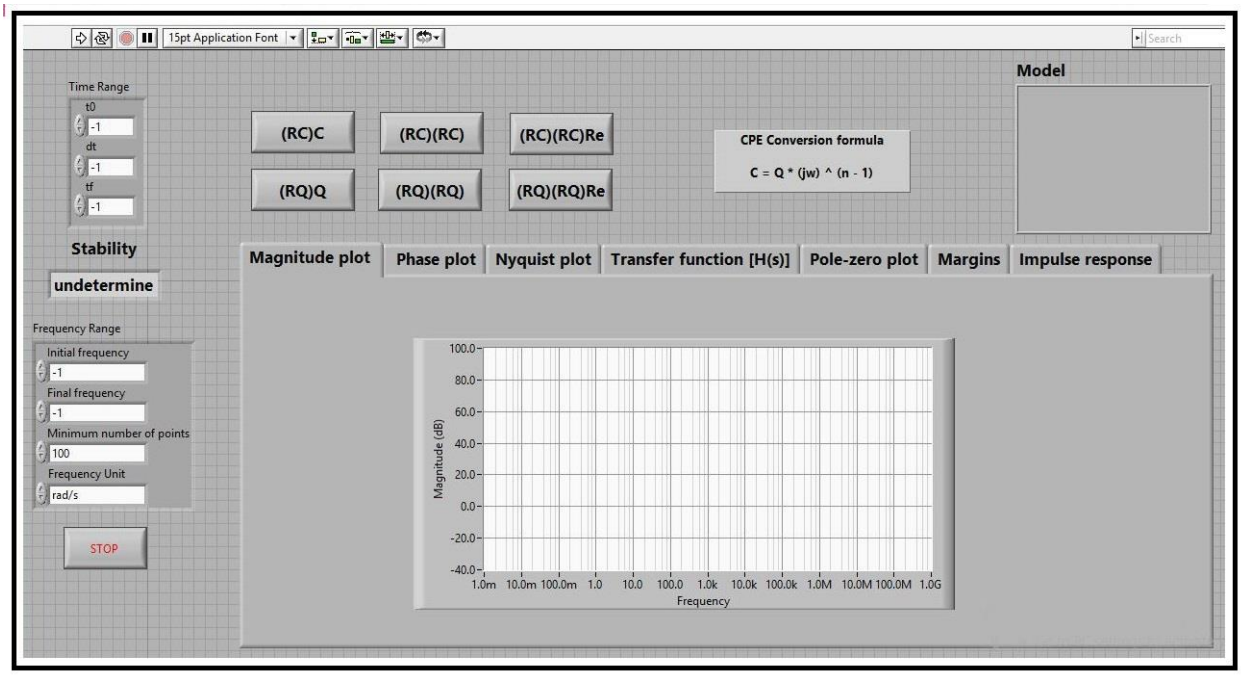

Figure. 10 Complete front panel of the developed program.

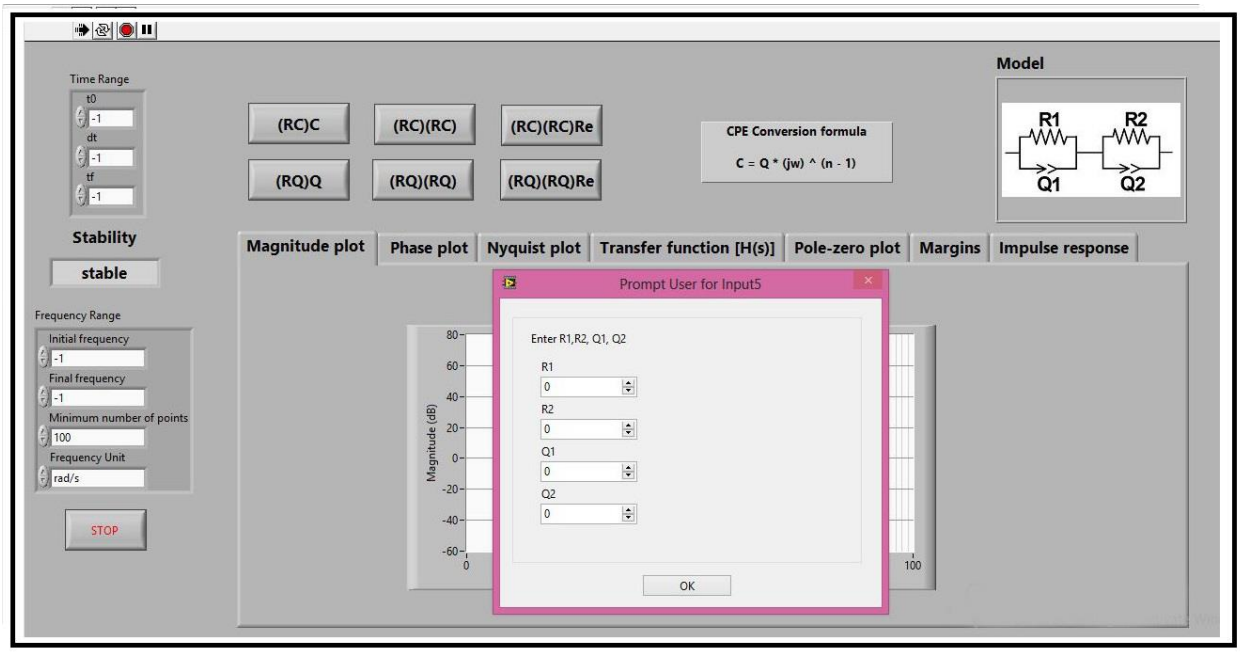

Fig. 11 Screenshot of the program with user dialogue box.

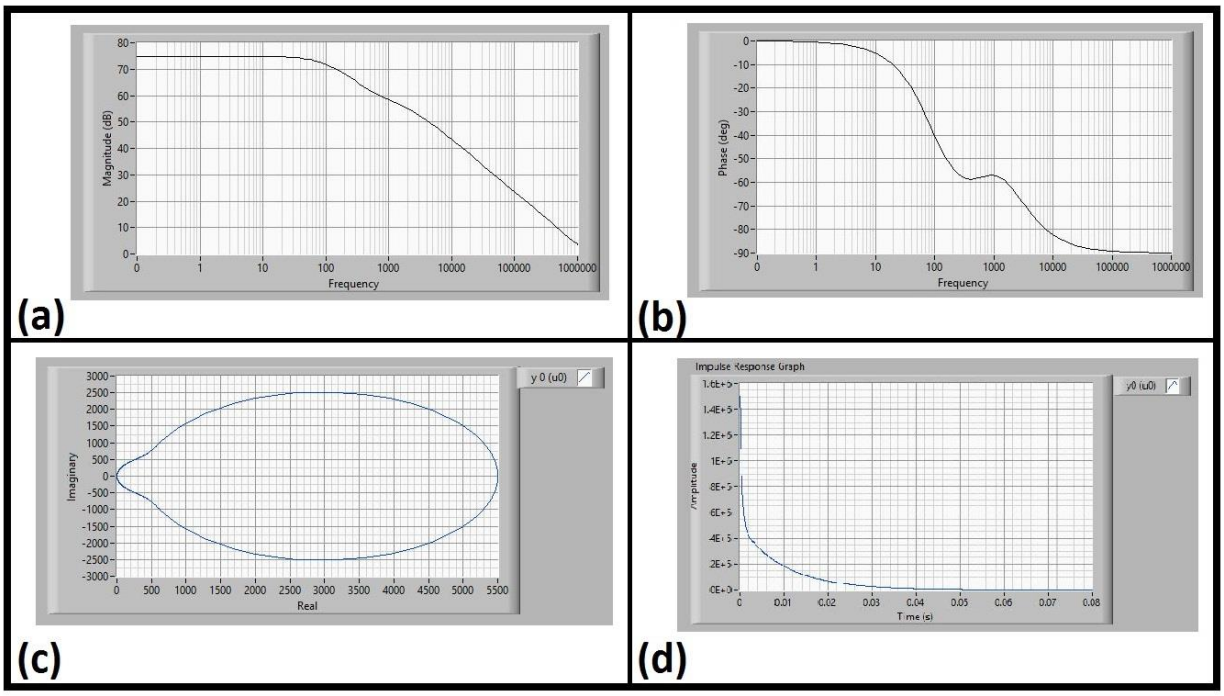

Figure. 12 The screenshot of the representative plots obtained by entering random set of values for (RQ)(RQ) model. (a) magnitude plot, (b) phase plot, (c) Nyquist plot, (d) impulse response.

4 Results and Discussions

4.1 Fabrication of electrodes

Thin layer of aluminium was deposited on glass substrate by vacuum vapor deposition technique. The electrodes were prepared such that the distance between two electrodes were 40 µm, 80 µm, 150 µm and 300 µm. The pictographs of the designed electrodes have been shown in fig. 13 (a-d). The distance between the electrodes edges were calculated using ImageJ software (National Institute of Health, US). The distance were found to be 40.13 µm, 82.26 µm, 150.93 µm and 316.53 µm. The micrographs of the electrode graphs have been shown in fig. 13 (e-h).

After the characterization of the electrodes, wells made using micropipette tips and were fixed onto the glass-slides such that the mid-point of the gap line (perpendicular line running through mid-point of the edges of the electrodes which are parallel to each other) forms center of the well. This has been shown in fig. 3 (i). The wells were fixed using PDMS. Thin copper strips were attached to the base of the electrodes. The copper strips were used as the junction points for connecting the electrodes with impedance analyzer.

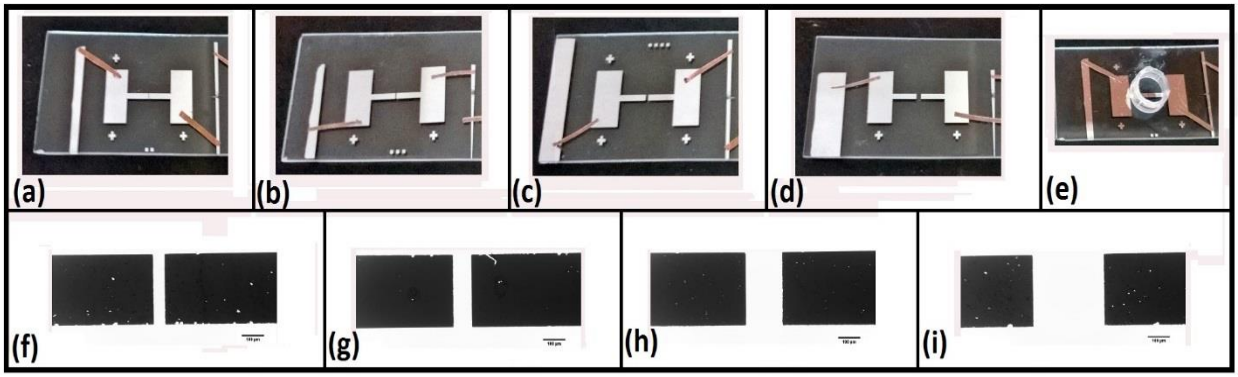

Fig. 13 The pictograph of electrodes with (a) E40, (b) E80, (c) E150 and (d) E300 , the micrograph of electrodes (f, g, h, i) and final structure with well (e).

4.2 Selection of the electrode system

(RQ)Q, (RQ)(RQ) and (RQ)(RQ)Re electrical models are the commonly used models which are used for the modelling of the biological samples. These models are mathematically represented, and by the equations 2 ((RQ)Q), 3 ((RQ)(RQ)) and 4 ((RQ)(RQ)Re) respectively. 'Q' is associated with constant phase element (CPE). CPE may be defined as a non-ideal capacitor and its reactance is given by equation 4. The 'n' value in the equation 5 is known as inhomogeneity constant. When n = 1, CPE behaves as an ideal capacitor. The 'Q' values, so obtained, were converted to equivalent 'C' (capacitor) values using equation 6. The calculated equivalent 'C' values were used for further analysis.

$$H(s) = \frac{1 + (RQ_1 + RQ_2)s}{Q_2 s + RQ_1Q_2s^2} \quad (2)$$

$$H(s) = \frac{(R_1 + R_2) + (R_1R_2Q_1 + R_1R_2Q_2)s}{1 + (R_1Q_1 + R_2Q_2)s + R_1R_2Q_1Q_2s^2} \quad (3)$$

$$H(s) = \frac{R_e(R_1 + R_2) + (R_1R_2R_eQ_1 + R_1R_2R_eQ_2)s}{(R_1 + R_2 + R_e) + (R_1R_2Q_1 + R_1R_2Q_2 + R_1R_eQ_1 + R_2R_eQ_2)s + R_1R_2R_eQ_1Q_2s^2} \quad (4)$$

$$X_Q = \frac{1}{(jw)^nQ} \quad (5)$$

$$C = (jw)^{n-1}Q \quad (6)$$

The values of these elements were obtained from the fitting of the experimental impedance profiles. The fitting was done by non-linear least square method using solver add-in in Excel 2013. The impedance analysis was done in the frequency range of 50 Hz-10 kHz. For the selection of the electrodes, 200 µl of distilled water was used for the analysis. The impedance profiles, their fit and the values of the calculated elements using different electrodes have been shown in fig. 14, 15 and 16.

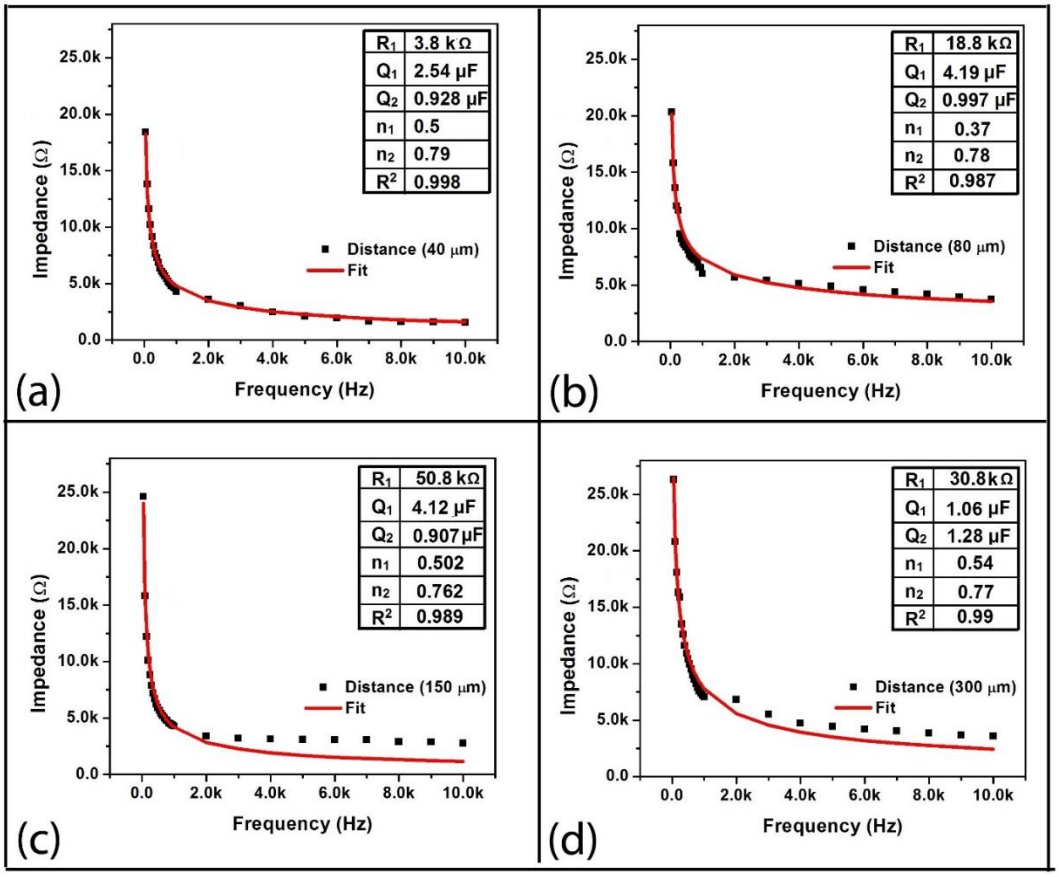

Fig. 14 Fitting of impedance profile using (RQ)Q model for (a) E40, (b) E80, (c) E150 and (d) E300.

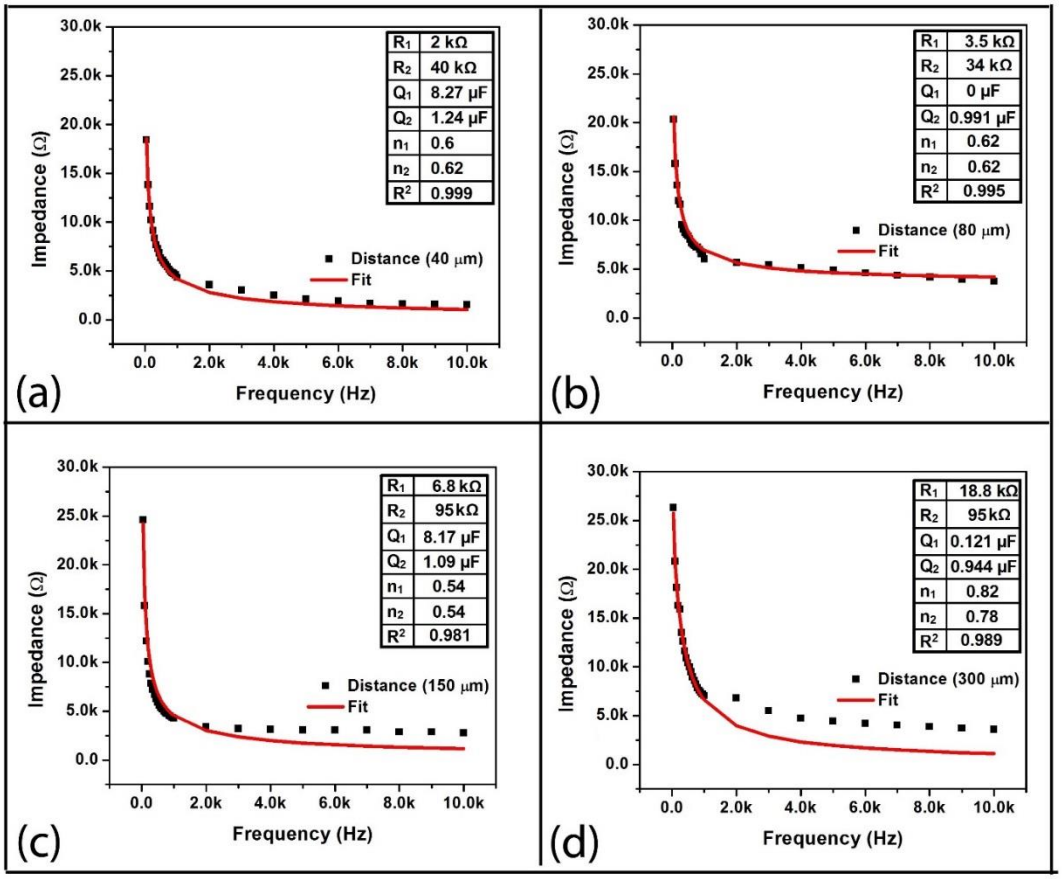

Fig. 15 Fitting of impedance profile using (RQ)(RQ) model for (a) E40, (b) E80, (c) E150 and (d) E300.

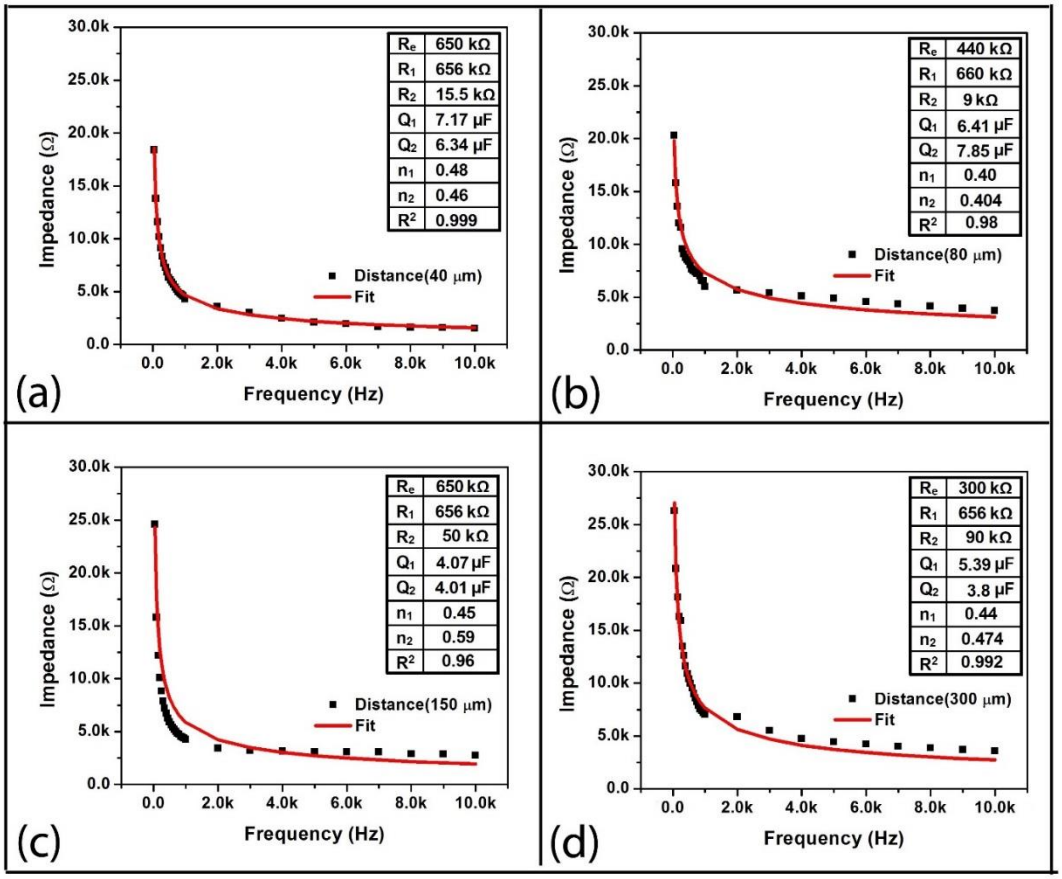

Fig. 16 Fitting of impedance profile using (RQ)(RQ)Re model for (a) E40, (b) E80, (c) E150 and (d) E300.

The values obtained from the modelling and the equivalent 'C' values were used as the input for the developed program. Impulse response, bode plot and Nyquist plot and of the equivalent electrical circuit models were obtained from the program. The time constant of the circuits were calculated from the impulse response by fitting impulse response profile. The fitting and dominant pole time constant was obtained using equation 7. Equation 8 was used for the obtaining two separate time constants using generalized approach.

$$y = Ce^{-pt}, C = \frac{\sigma w}{\sigma^2 + w^2} \text{ and } T_d = 1/p \quad (7)$$

$$y = A + C_1 e^{-t/T_1} + C_2 e^{-t/T_2} \quad (8)$$

The impulse responses of the electrode systems obtained form (RQ)Q, (RQ)(RQ) and (RQ)(RQ)Re have been shown in fig. 17, 18 and 19. The (RQ)(RQ) and (RQ)(RQ)Re models showed zero residual amplitude values for all the electrode systems In this models, two time constants were observed. The fitting correlation coefficient of the (RQ)(RQ) and (RQ)(RQ)Re models were equal to 1. Based on the impulse response, the (RQ)Q model was rejected as the residual amplitude of the impulse response was a non-zero entity. (RQ)(RQ) model showed time constants of lower values compared to (RQ)(RQ)Re model. Electrical systems with lower time constants is regarded as comparatively more stable. Hence (RQ)(RQ) model was selected for further analysis.

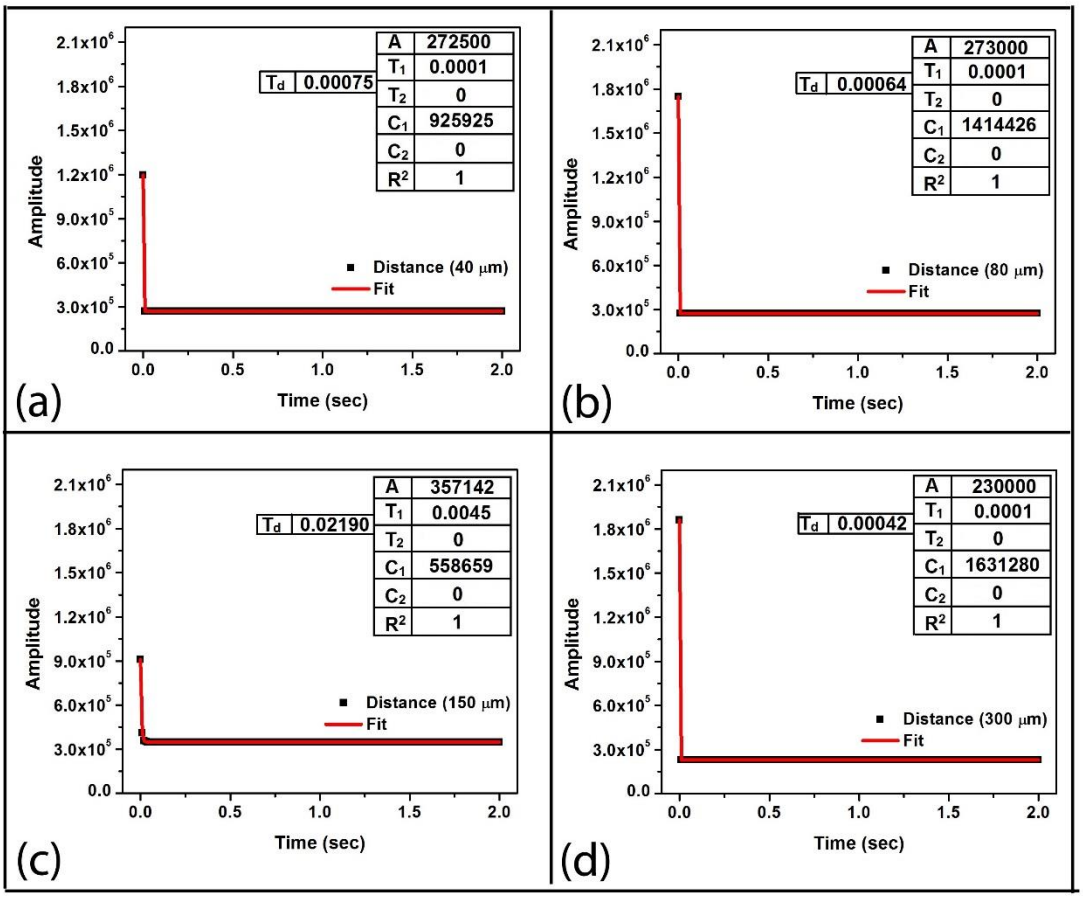

Fig. 17 Fitting of impulse response profile of (RQ)Q model. (a) E40, (b) E80, (c) E150 and (d) E300.

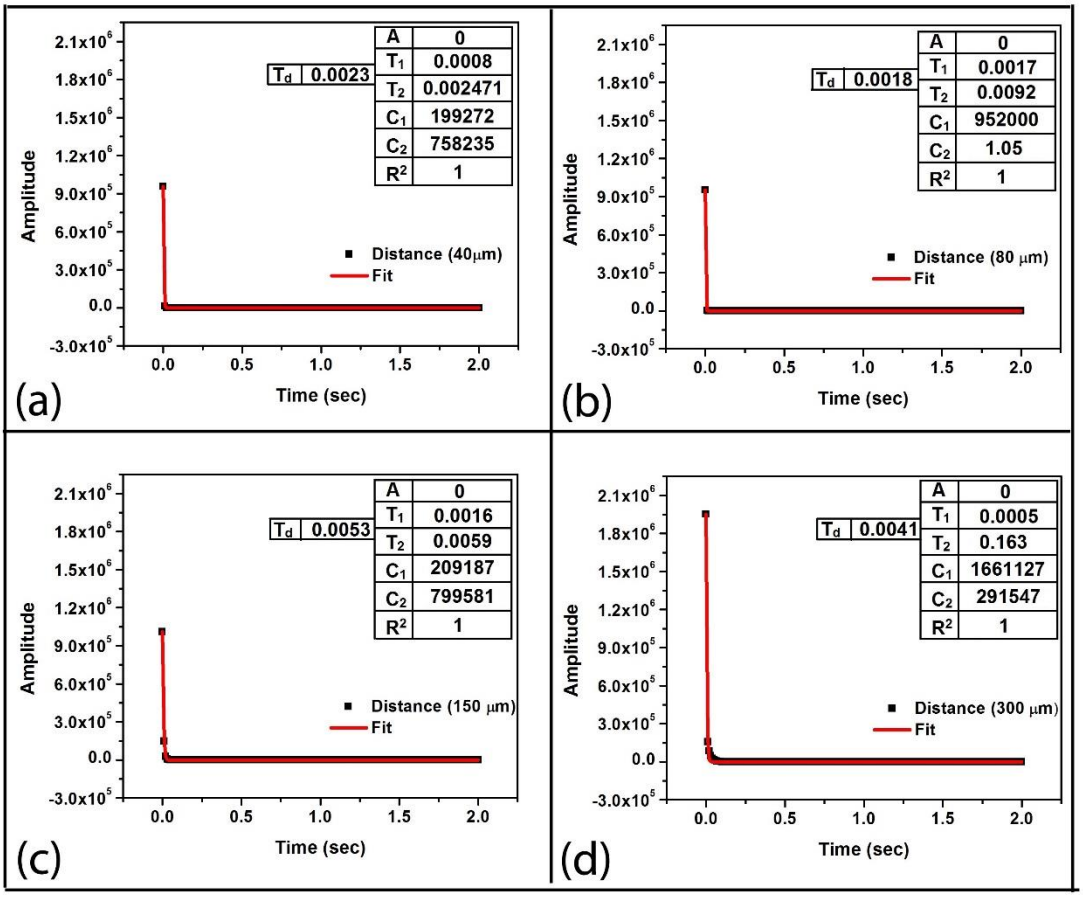

Fig. 18 Fitting of impulse response profile of (RQ)(RQ) model. (a) E40, (b) E80, (c) E150 and (d) E300.

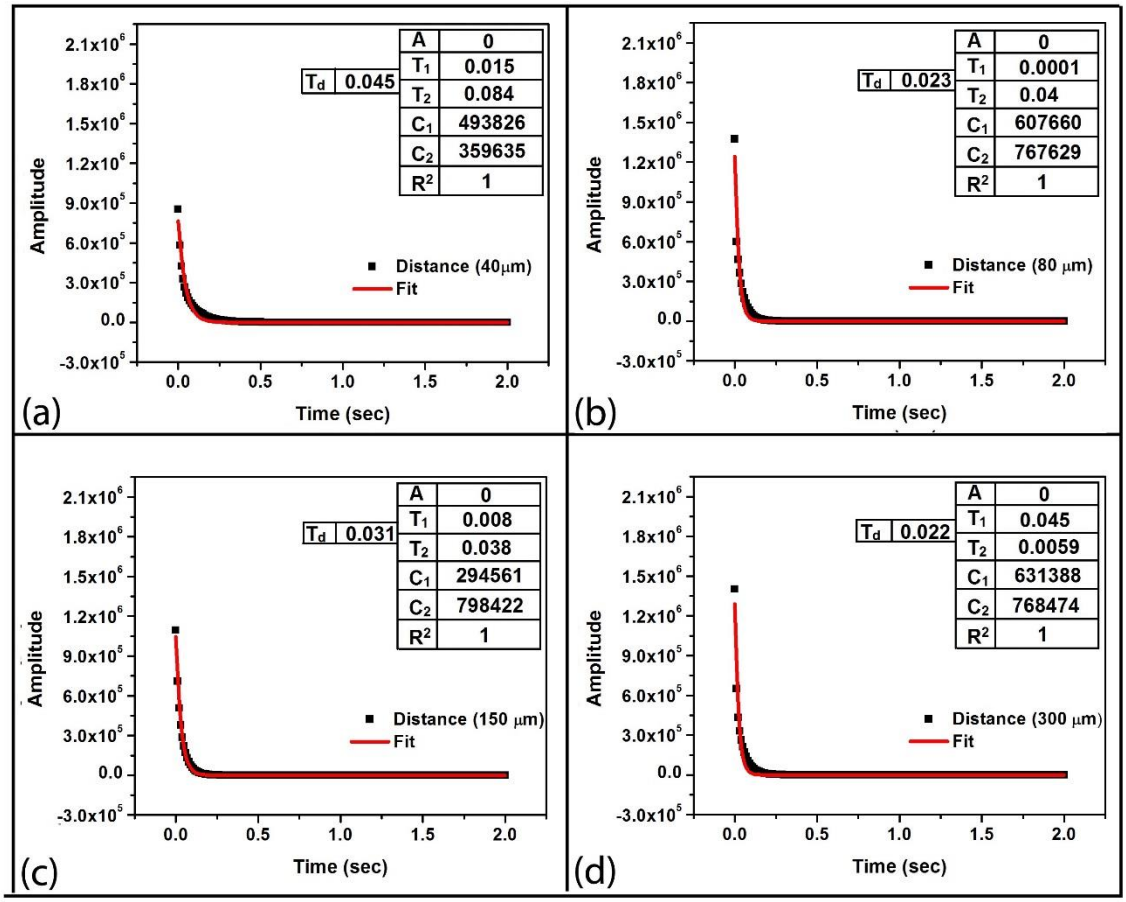

Fig. 19 Fitting of impulse response profile of (RQ)(RQ)Re model. (a) E40, (b) E80, (c) E150 and (d) E300.

Careful examination of the relaxation constants and the fitting parameters suggested that, E40 electrode system was the most stable system. Hence, E40 electrode system was used for further analysis.

4.3 Analysis of distilled water

The Nyquist plots of all the electrode systems using distilled water (DW) as an analyte has been shown in fig. 20, fig. 21 and fig. 22 for (RQ)Q, (RQ)(RQ) and (RQ)(RQ)Re models respectively. The Nyquist plot obtained from (RQ)Q model showed an initiation of a semicircular region. In neither of the cases, the semicircle was completed. Instead, there was a spike having slopes of different magnitudes. The occurrence of the spikes has been related to the imperfections present in the electrodes which result in the altered electrical phenomenon (faradaic current) at the sample electrode interface. This type of phenomenon is undesirable for any electrochemical impedance analysis.

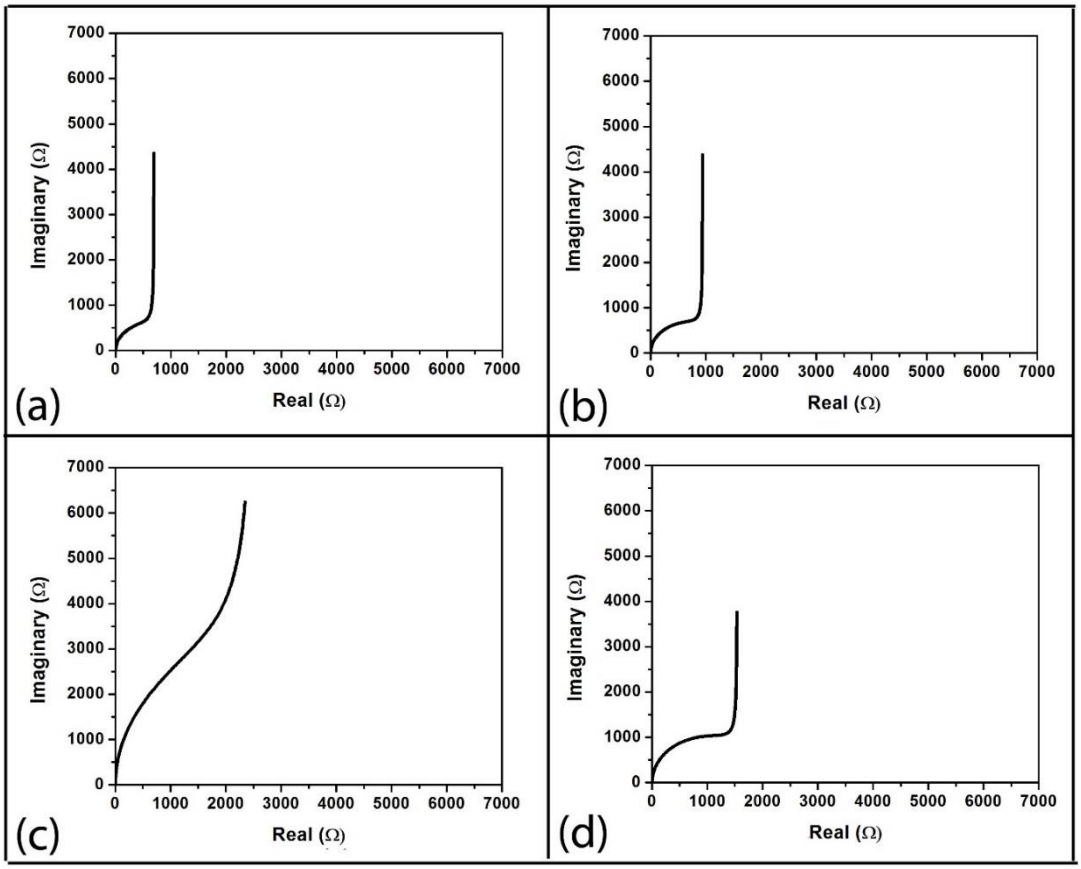

Fig. 20 Nyquist plot of (RQ)Q model. (a) E40, (b) E80, (c) E150 and (d) E300.

The Nyquist plot for the (RQ)(RQ) model showed formation of semicircles when E40, E80 and E150 electrodes were used, even though, there are two constant phase elements (CPEs) present in the circuit. On the contrary, when E300 electrode was used, a combination of two semicircles was seen. This indicated that the time constants of the two CPEs might be significantly different. The bulk resistance was found to be 2100 Ω, 1875 Ω and 5090 Ω respectively for E40, E80 and E150 electrode systems. The bulk resistance of E300 electrode system could not be calculated for the plots due to bulk property, and electrical double layer were merged. The combination of the bulk and the faradaic resistances was ~5690 Ω. The sample resistance (R_∞)(resistance at high frequency) was found to be zero when E40, E150 and E300 electrode systems were used. R_∞ for the E80 system was 175 Ω. This suggested that the resistance of the distilled water was ~175Ω.

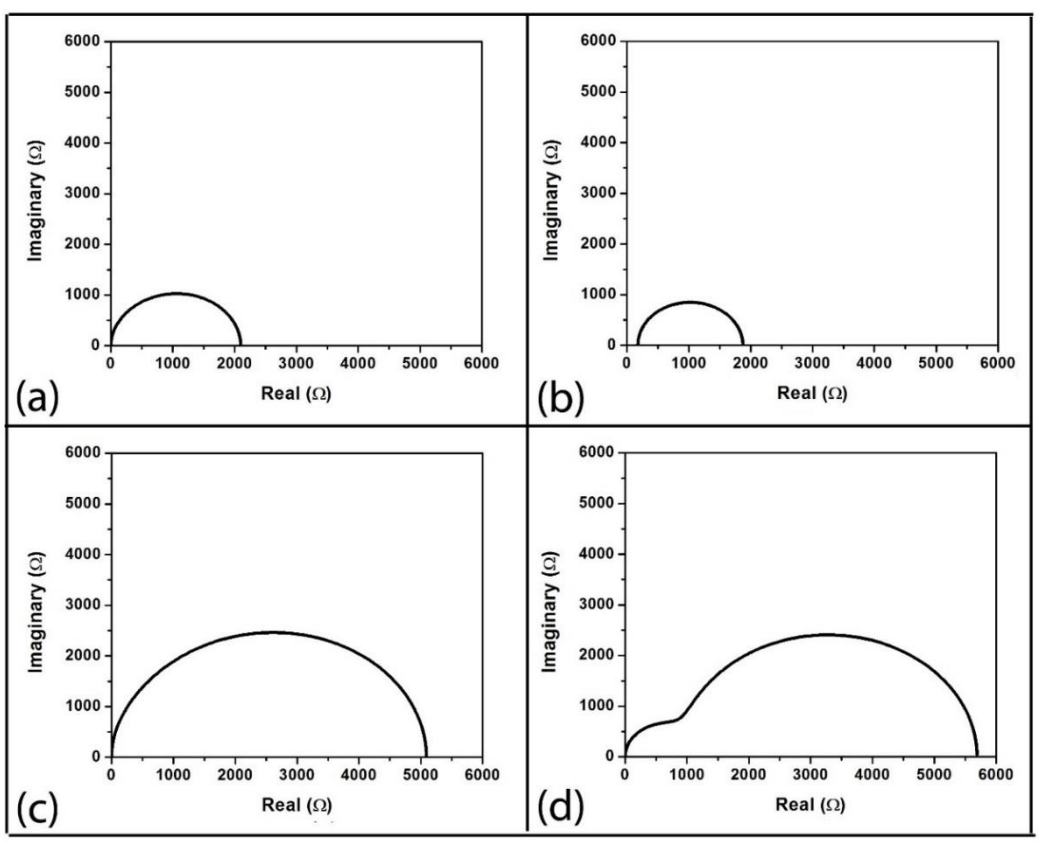

Fig. 21 Nyquist plot of (RQ)(RQ) model. (a) E40, (b) E80, (c) E150 and (d) E300.

The Nyquist plots of the (RQ)(RQ)Re model also showed profiles that could be due to the presence of CPEs of distinctly different time constants. Unlike in the Nyquist plot of (RQ)(RQ) model of E300, the two semicircular regions were not distinctly visible. The initial semicircular regions appeared as bulges to the more prominent semicircular plots (marked by arrows). Similar to the (RQ)(RQ) model, the combination of the bulk and the faradaic resistances was noted from the Nyquist plot for (RQ)(RQ)Re model. The combination of the bulk and faradaic resistances was 38.2 kΩ, 31.1kΩ, 33.5 kΩ and 33.2 kΩ for E40, E80, E150 and E300 systems respectively.

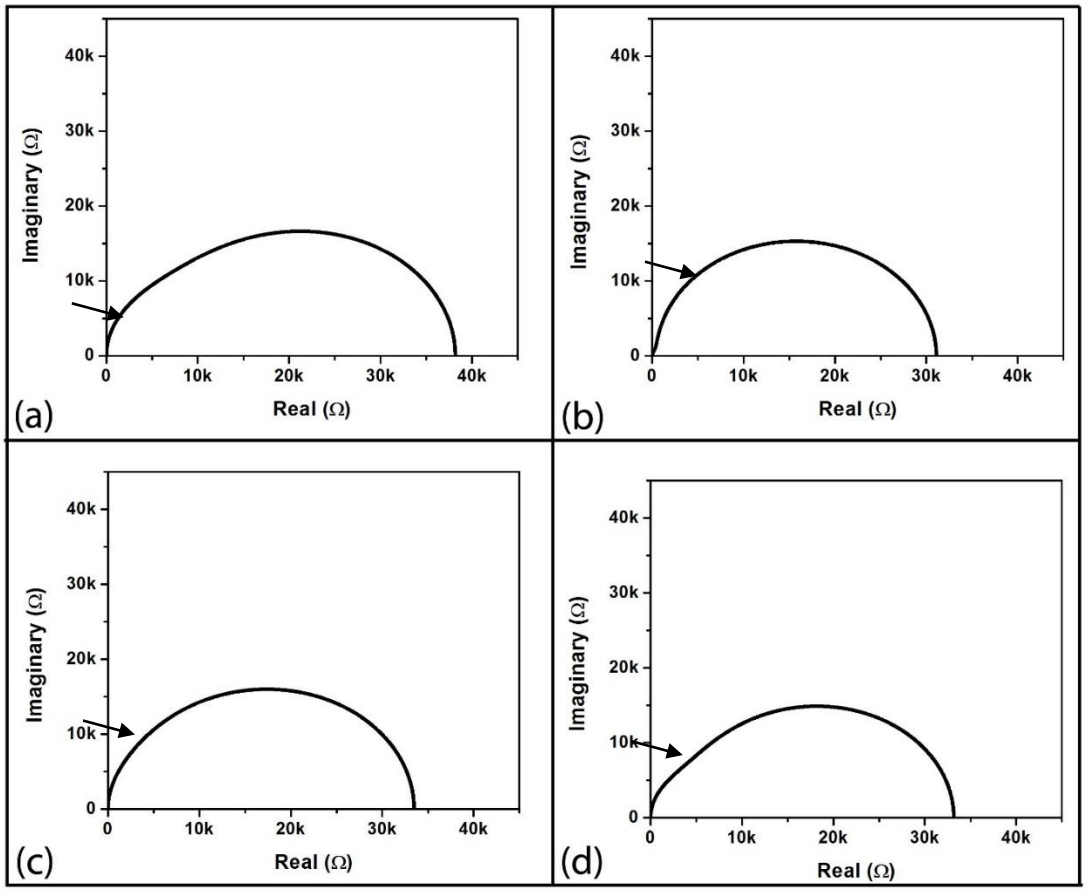

Fig. 22 Nyquist plot of (RQ)(RQ)Re model. (a) E40, (b) E80, (c) E150 and (d) E300.

The bode plots of different models has been shown in fig. 23, fig. 24 and fig. 25 respectively for (RQ)Q, (RQ)(RQ) and (RQ)(RQ)Re models respectively. The amplitude profiles of the (RQ)Q model was similar for all the electrode systems. The phase profiles

for all the electrode systems showed Gaussian profile with a distinct peak. The phase profiles of the E40, E80 and E300 electrode systems showed a peak maxima at ~75 Hz, whereas, the peak maxima for E150 electrode system was at ~30 Hz. The phase margin for the E40, E80, E150 and E300 electrode system was found to be 90.049, 90.0434, 90.0085 and 90.0286 respectively. The electrode systems showed three distinct regions. In the low frequency region, there was a decrease in the magnitude response. Thereafter, the decrease in the amplitude response was slow in the mid frequency region due to the presence of capacitive element, confirmed from the phase plot which shows a phase of -90^{o}. Subsequently the magnitude plot again decreased monotonically with steeper slope at high frequency region. The magnitude plot of E150 showed only two distinct regions. In the low frequency region, the steepness of the magnitude plot was slower as compare to the steepness in the high frequency region.

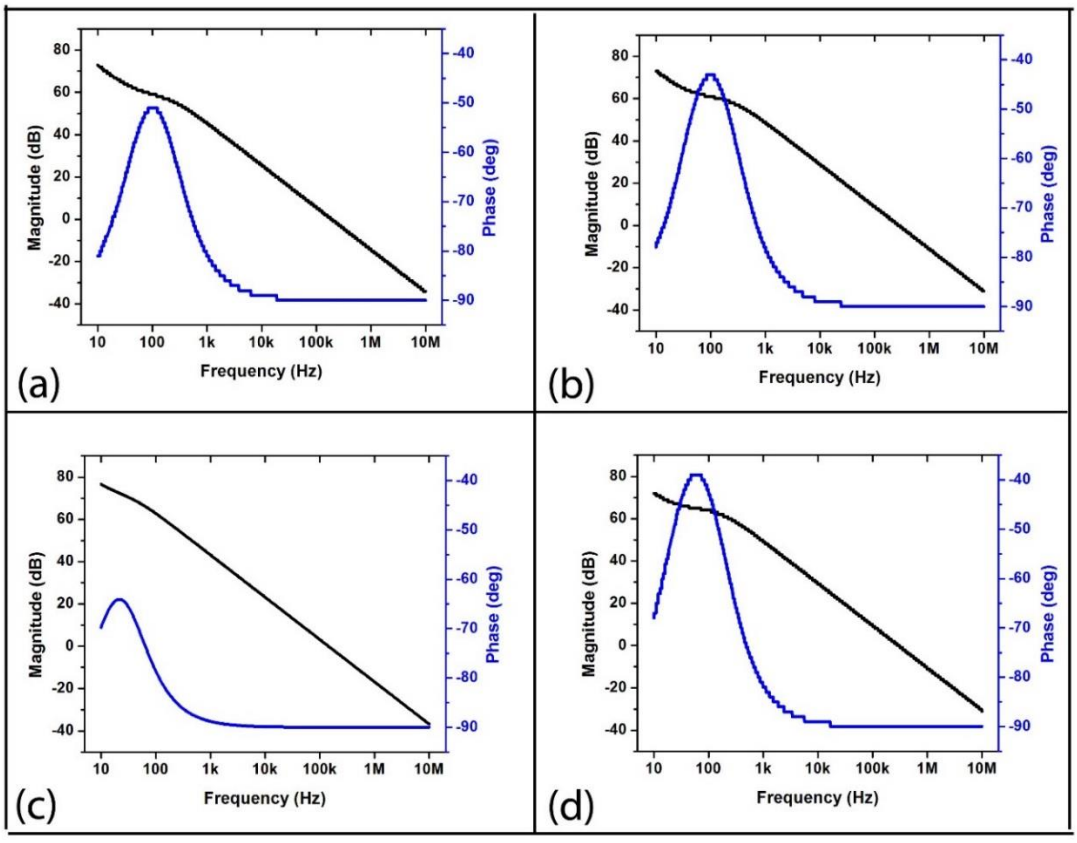

Fig. 23 Bode plots of (RQ)Q model for (a) E40, (b) E80, (c) E150 and (d) E300.

The bode plot of the electrode system fitted with (RQ)(RQ) model has been shown in fig 13. The magnitude response of the E40 and E150 electrode system showed two regions. The initial part of the magnitude response was a constant region. This region was followed by a monotonically decreasing amplitude region in the higher frequency range. The amplitude plot of E80 electrode system showed three distinct regions. In the low and the high frequency region, amplitude response was constant and was parallel to the frequency axis. In the mid frequency region, there was a decrease in the amplitude response. The E300 electrode system also showed three distinct regions but, its profile was completely different than E80 electrode system. The amplitude response was steeply decreasing in the low and the high frequency region as compare to the mid frequency region. The phase response of the E40 and E300 systems showed the tendency of attaining a peak in the flat amplitude response region. This indicated the probability of presence of capacitive element in the circuit. This was confirmed from attainment of a -90^{o} phase at higher frequencies. The phase response of E80 electrode system showed a valley in the mid frequency region where there was a decrease in the amplitude profile. This indicated the presence of capacitive element in the circuit. It would be wise to mention over here that during modelling of impedance profile, Q_2 was found to be zero. Due to this reason, this type of plot was obtained. In the E300 electrode system, a peak in mid frequency region was observed. The phase profile reached a -90^{o} phase at higher frequencies.

The bode plots of the (RQ)(RQ)Re model have been shown in fig. 14. E40, E150 and E300 electrode system showed two regions. In the initial region, there was a slow decrease in the amplitude response. Thereafter, there was a steep decrease in the amplitude at in the mid and the high frequency region. In all the three systems, the phase at lower frequencies was higher which decreased to a residual value at high frequency region. The amplitude response of E80 electrode system showed three distinct regions. In the low and the high frequency regions, there was a steep decrease in the amplitude response. In the mid frequency region, the steepness of decrease in the amplitude response was slower. The phase response of the system showed a peak in the mid frequency region, which subsequently attain a residual value at high frequency region.

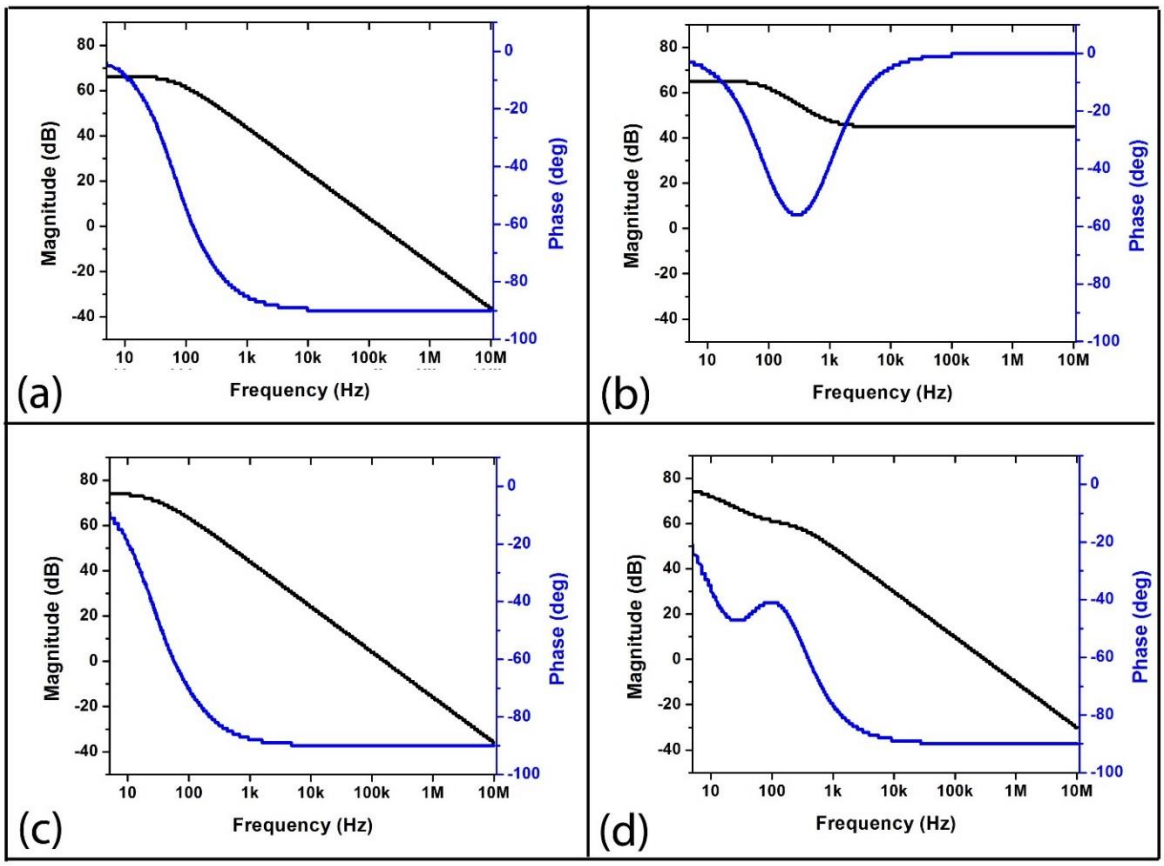

Fig. 24 Bode plots of (RQ)(RQ) mode for (a) E40, (b) E80, (c) E150 and (d) E300.

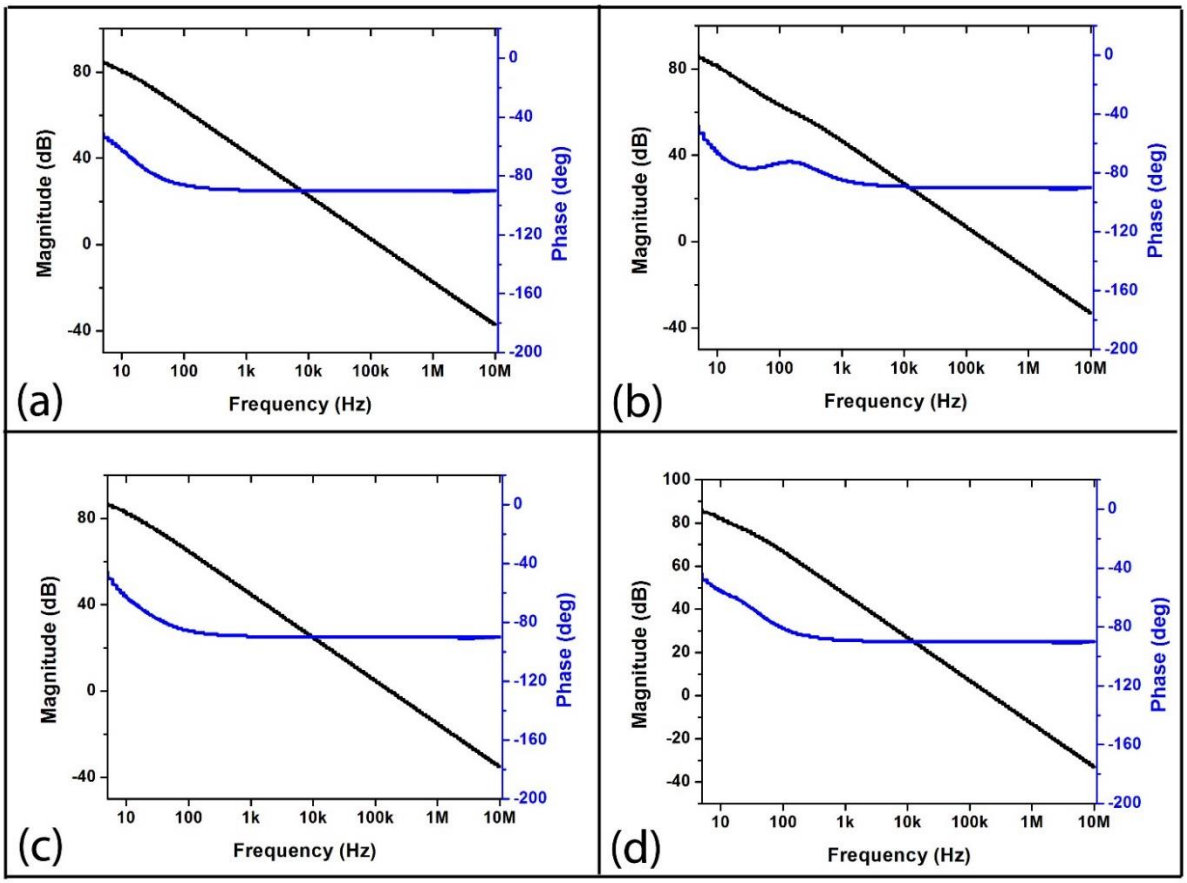

Fig. 25 Bode plots of (RQ)(RQ)Re model for (a) E40, (b) E80, (c) E150 and (d) E300.

4.4 Analysis of saline solution

Saline solutions of different strengths were analyzed using the (RQ)(RQ) model using E40 electrode system. The impedance profile of the samples have been shown in fig. 26. The experimental data was fitted using (RQ)(RQ) mathematical model. The values of the electrical elements were calculated. R, R_1 and Q_1 were found to be lowest in S1. An increase in the strength of saline solutions in S2, S3 and S4 did not alter the R, R_1 and Q values of the samples. An increase in the strengths from S2 to S3 resulted in the increase Q_1 value. A further increase in the saline strengths in S4 did not show any alteration in Q1 values as compare to S3. The CPE inhomogeneous constants (n and n_1) were equal in all the samples. The results over here suggested that the capacitive elements (due to both sample and electrical double layer) were behaving as non-ideal capacitors.

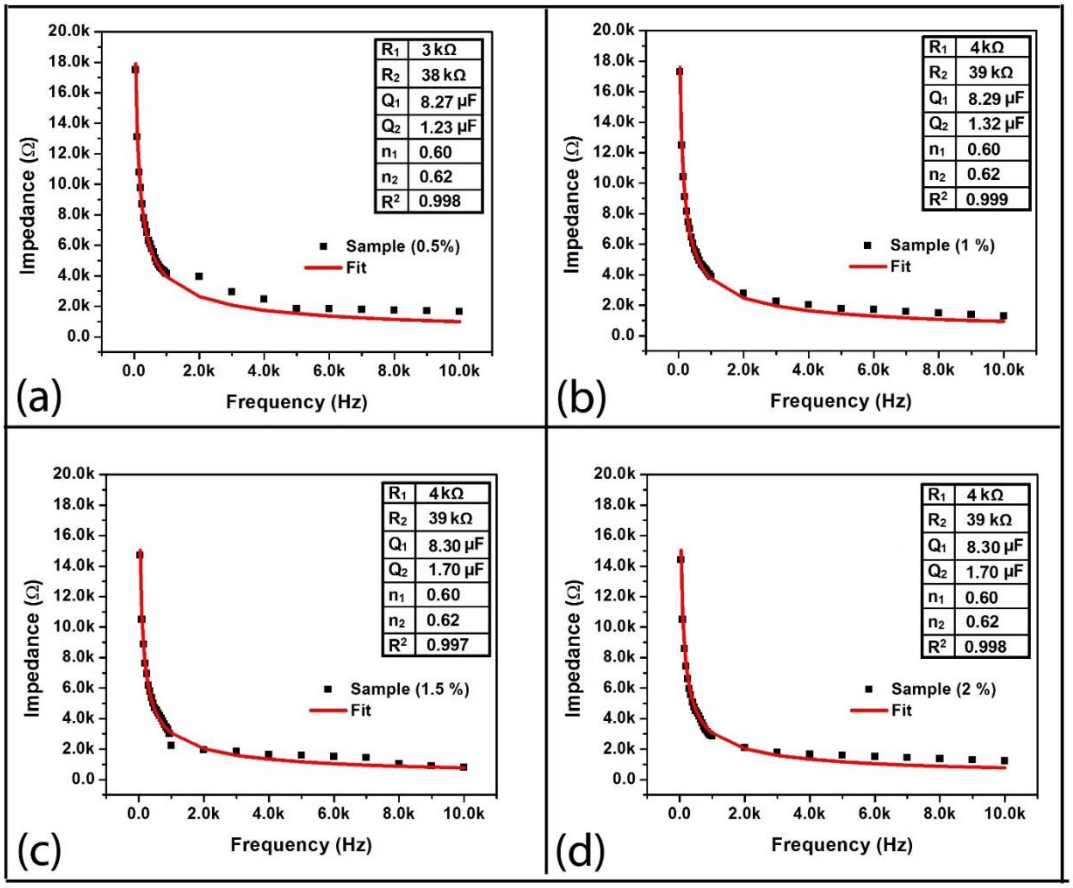

Fig. 26 Impedance profiles of E40 electrode system. (a) S1, (b) S2, (c) S3 and (d) S4.

The impulse response profile of the samples have been shown in fig. 27. The impulse response profile was fitted using the previously mentioned mathematical model (equation 5). The time constants of the circuits were calculated. The differences amongst the time constants within the samples and amongst the samples were not distinctly different. This suggested that the electrical properties of the samples would behave in a similar manner.

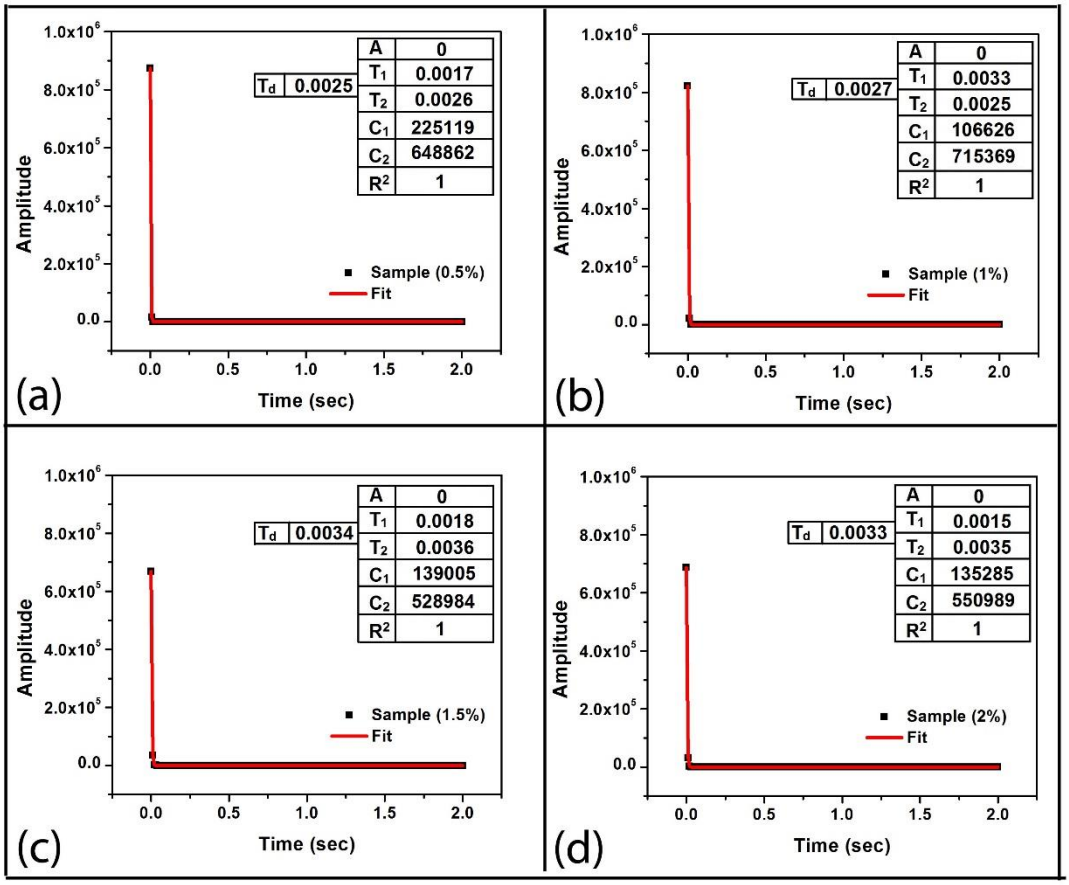

Fig. 27 Impulse response profiles of E40 electrode system for (a) S1, (b) S2, (c) S3 and (d) S4.

The Nyquist plot of the samples has been shown in fig. 28. All the samples showed a similar semicircular profiles. From the graph, it can be observed that the semicircular profile intersected at 0 Ω. This suggested that the resistance of the solution at high frequency is 0 Ω. Even though there are two capacitive elements present in the circuit, additional semicircle or bulges were not observed. This can be explained by the relaxation times of the capacitive elements. The changes in the relaxation times of the capacitive elements were insignificant. The presence of similar type of Nyquist profile of the sample can be explained by the absence of the activation controlled process. Since there are no changes in the rate of reaction of the samples during the analysis, the potential changes in the presence of the samples was mainly due to the formation of the electrical double layer across the electrode surfaces.

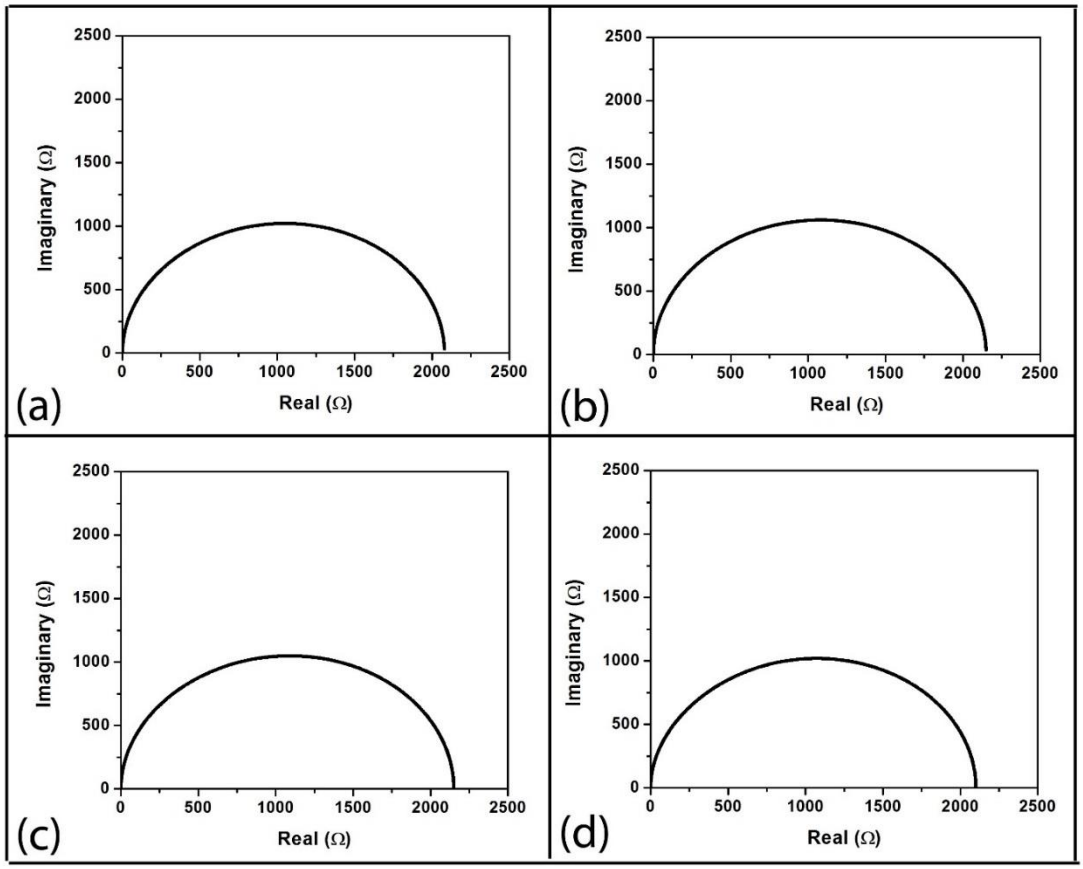

Fig. 28 Nyquist plots of E40 electrode system for (a) S1, (b) S2, (c) S3 and (d) S4.

The bode plots of the sample has been shown in fig. 29. Similar to the Nyquist plot, bode plots of all the samples were found to be similar. The amplitude profiles of all the samples showed two distinct regions. In the low frequency region, the amplitude response was constant. An increase in the frequency resulted in the monotonically decrease in the amplitude plot. At lower frequencies, the phase component was highest, which rapidly decreased to a constant value of -90^{o} at higher frequencies. This indicated the presence of capacitive element within the circuit. The occurrence of similar plots in all the cases also suggested that the variation in the bode plot was not due to the variation in the sample concentration, but due to a constant parameter of the electrode system. This confirmed that, when E40 electrode system was used, the electrode polarization effect hampered the sample analysis.

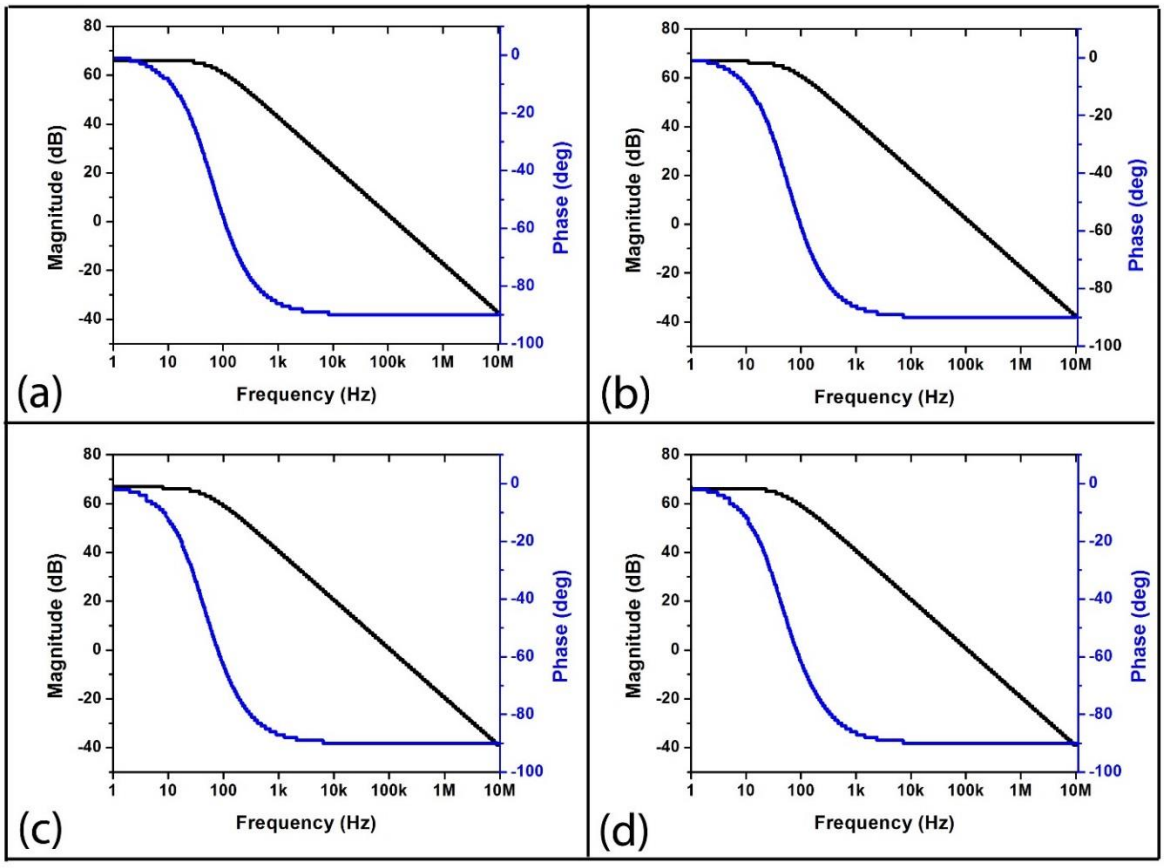

Fig. 29 Bode plots of E40 electrode system for (a) S1, (b) S2, (c) S3 and (d) S4.

4.5 Application of EIS stability analysis

For the purpose of application of this technique, four gel based samples were selected. Gelatin, corn starch, soluble starch and boiled starch were selected. The samples were named GH, CS, SS and BS respectively. The (RQ)(RQ) model was used to fit the impedance data as per previous explanation. The fitted impedance profiles of the samples with model parameters has been shown in fig. 30. From the component values obtained from fitting, it was found that all the samples showed small variation in R_1, R_2 and Q_2 values. The value of inhomogeneous constant n_2 for the samples GH, SS and BS was found to be comparable. The n_2 for the sample was nearly equal to zero which suggests that the component Q_2 for the sample using CS was behaving as an inductor.

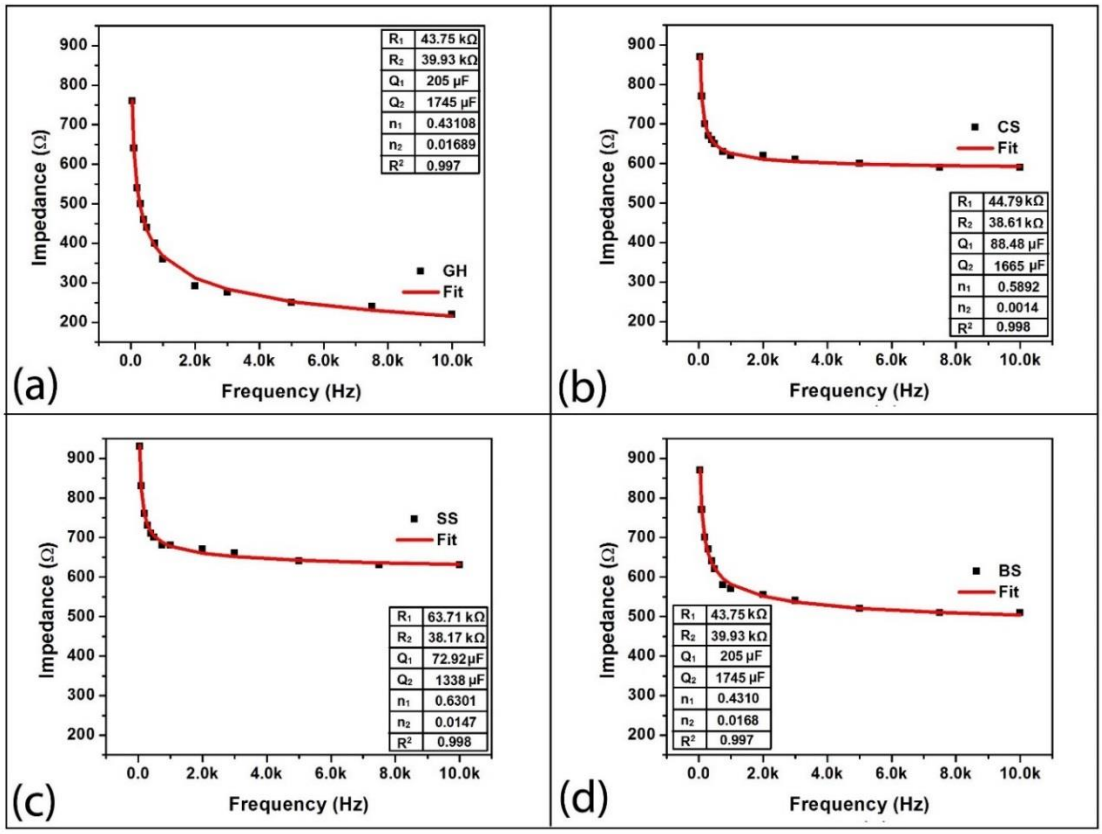

Fig. 30 Fitted impedance profiles with model parameters. (a) GH, (b) CS, (c) SS, (d) BS.

The impulse response and the values of the time constants for the samples has been shown in fig. 31. All the samples showed two time constants with zero residual amplitude. For the samples BS and CS, the time constants were similar. Two distinct time constants were obtained from the impulse profiles of the samples using SS and GH. The decay time for the sample SS was found to be least compare with other samples.

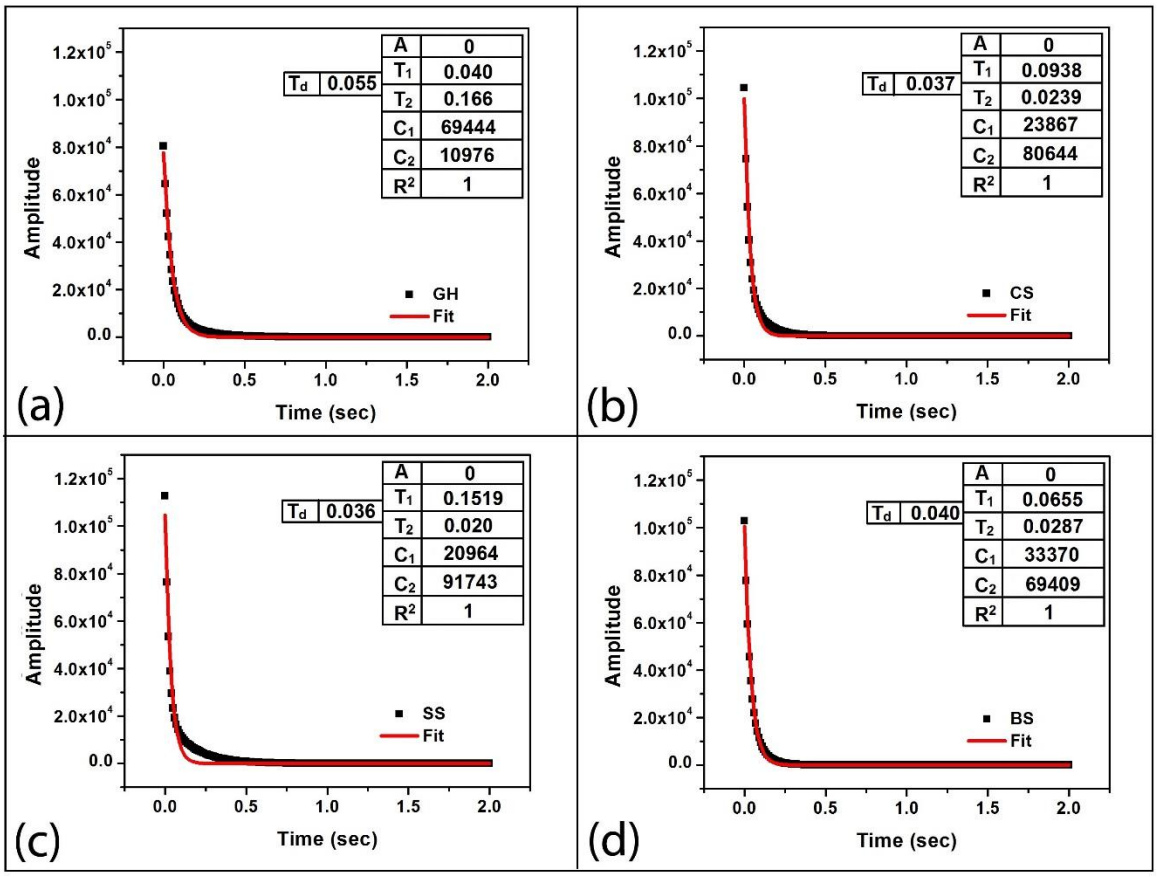

Fig. 31 Fitted impulse response profiles with model parameters. (a) GH, (b) CS, (c) SS, (d) BS

The Nyquist plot of the samples has been shown in fig. 32. When the samples BS and CS were used, the Nyquist plot showed formation of semicircles. For the samples SS and GH, a combination of two semicircles was seen. The bulk resistance for BS and CS was found to be 4183 Ω and 4169 Ω respectively. The combination of the bulk and faradaic

resistances for the samples SS and GH was found to be 5093 Ω and 4634 Ω respectively. For the sample SS, the effect of faradaic resistance was more prominent. This can be explained by looking at the values of the time constants of each sample. On the other hand, the effect of the bulk resistance was more pronounced in case of the sample GH. The high frequency resistance was zero for all the samples.

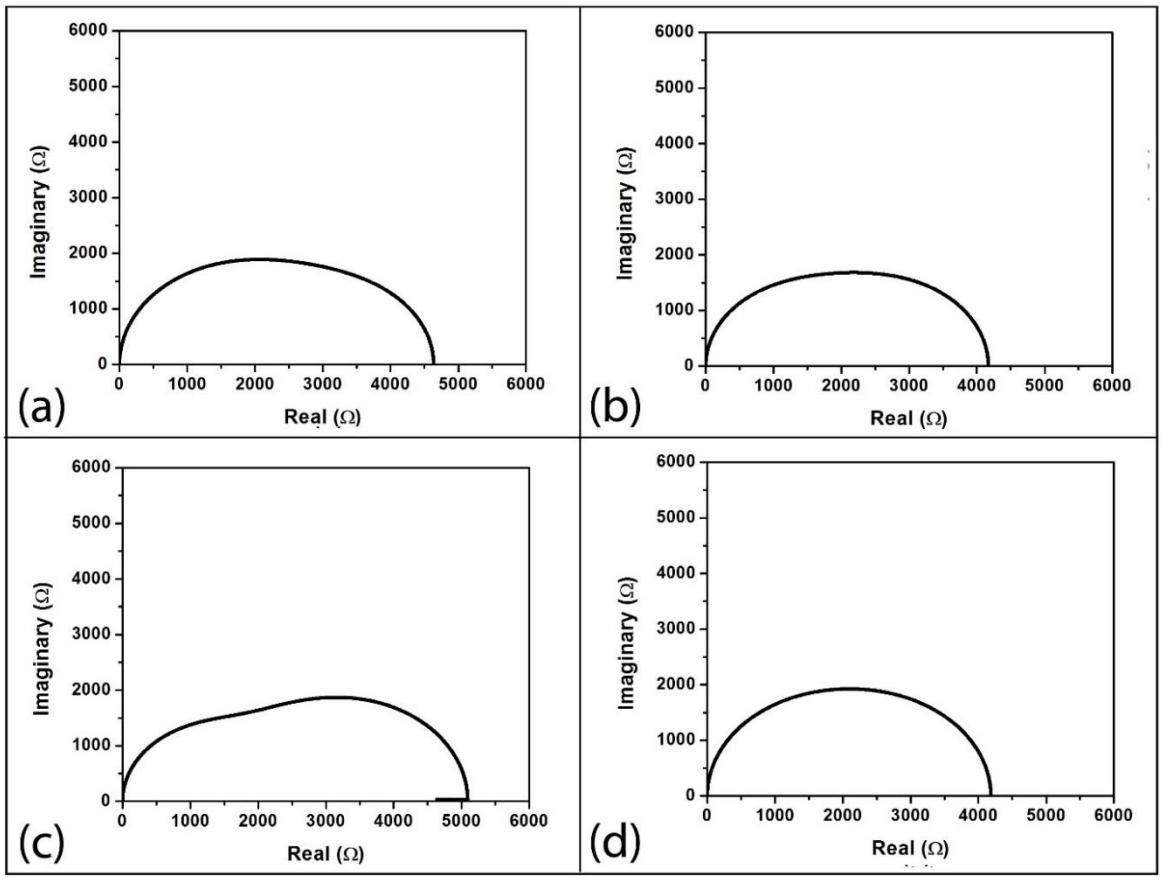

Fig. 32 Nyquist plots. (a) GH, (b) CS, (c) SS, (d) BS.

The bode plots for the samples BS, CS, SS and GH has been shown in fig. 33. Bode plots of all the samples were found to be similar. The magnitude response for all the samples showed two distinct regions. The amplitude response was constant for low frequency region. As frequency was increased, there was steep decrease in the amplitude response. The phase response for the samples BS and CS was monotonically decreased after -10^{o}. In the contrary, the samples SS and GH showed steep decrease in the phase

response after -20^{o} phase was reached in mid frequency range. At high frequencies, the phase response for all the samples was found to be equal to -90^{o}.

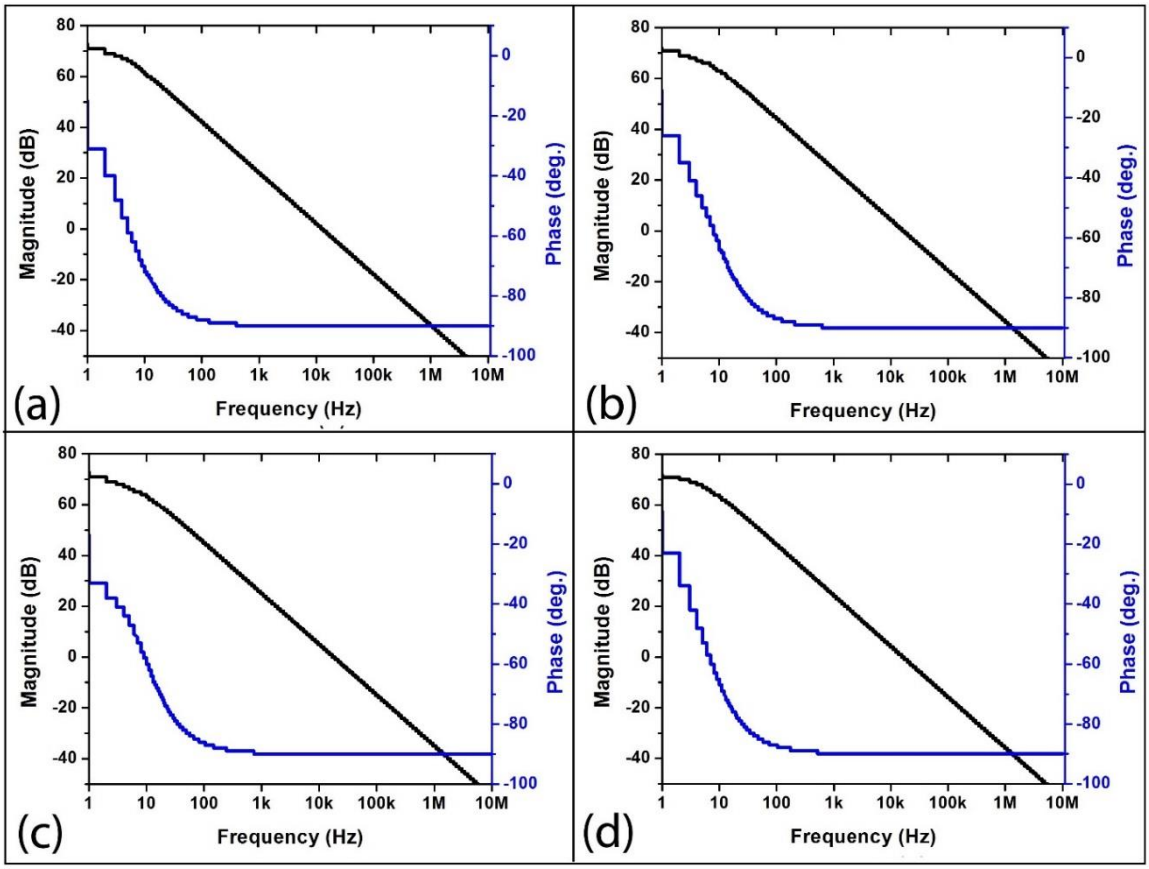

Fig. 33 Bode plots. (a) GH, (b) CS, (c) SS, (d) BS.

5 Conclusion and future scope

5.1 Conclusion

EIS is found to be useful for the analysis of bipolar impedance based sensor. With the help of EIS, it is possible to obtain in-depth information about interactions at sensor-electrolyte interface. LabVIEW based program is designed successfully and utilized in determining the stability analysis of the impedance based sensor. The best equivalent model ((RQ)(RQ)) for sensor-electrolyte interface is defined using curve fitting method. Most stable electrode system is found out to be E40. The stable system is confirmed using the stability analysis. The analysis of the saline solution of different strengths is carried out successfully using E40. For the purpose of the application, gel samples are also analyzed using (RQ)(RQ) model.

5.2 Limitation of current design

The stability of the sensor needs to be increased. The analysis is limited to the samples in liquid form. There is involvement of many manual calculations in the process of overall analysis, which is time-consuming.

5.3 Future scope

With the advanced sensor design, it is possible to analyze many samples of biological importance. The sensitivity can be increased by using coatings of novel metals. The LabVIEW program can be modified to obtain the best fit and most stable sensor parameters automatically. Also, the conversion of CPE to equivalent C in LabVIEW program can save a lot of calculations. The system can be made more portable by replacing the function generator with IC. The use of Arduino or any microcontroller based interface with LabVIEW helps in direct EIS data acquisition.

Bibliography

[1] Chen, Y. (1999). EIS measurement for corrosion monitoring under multiphase flow conditions. *Electrochimica Acta, 44*(24), 4453-4464.

[2] Daniels, J. S. (2007). Label-Free Impedance Biosensors: Opportunities and Challenges. *Electroanalysis*, 1239-1257.

[3] Grieshaber, D. (2008). Electrochemical Biosensors - Sensor Principles and Architectures. *Sensors*, 1400–1458.

[4] Ivnitski, D. (1999). Biosensors for detection of pathogenic bacteria. *Biosensors and Bioelectronics, 14*(7), 599-624.

[5] Koncki, R. (2007). Recent developments in potentiometric biosensors for biomedical analysis. *Analytica Chimica Acta, 599*(1), 7-15.

[6] Liu, Q. (2009). Impedance studies of bio-behavior and chemosensitivity of cancer cells by micro-electrode arrays. *Biosensors and Bioelectronics, 24*(5), 1305-1310.

[7] Macdonald, J. R. (2005). *Impedance Spectroscopy: Theory, Experiment, and Applications, 2nd Edition.* wiley.

[8] Muralidharan, p. V. (n.d.). *Researchgate*. Retrieved from http://www.researchgate.net/post/Can_someone_explain_the_meaning_of_activation_controlled_or_diffusion_controlled_reactions

[9] Park, S. (2006). Electrochemical non-enzymatic glucose sensors. *Analytica Chimica Acta, 556*(1), 46-57.

[10] Romero-Castañón, T. (2003). Impedance spectroscopy as a tool in the evaluation of MEA's. *Journal of Power Sources, 118*(1), 179-182.

[11] Scully, J. R. (1993). *Electrochemical Impedance: Analysis and Interpretation.* ASTM.

[12] Sekar, N., & R.P., R. (2013). Electrochemical impedance spectroscopy for microbial fuel cell characterization. *Journal of Microbial and Biochemical Technology, 5*((S6) pp. S6-004).

[13] Thévenot, D. R. (2001). Electrochemical biosensors: recommended definitions and classification. *Biosensors and Bioelectronics, 16*(1-2), 121–131.

[14] Wang, J. (2006). Electrochemical biosensors: Towards point-of-care cancer diagnostics. *Biosensors and Bioelectronics, 21*(10), 1887-1892.

[15] Yoo, J.-S. (2003). Peer Reviewed: Electrochemical Impedance Spectroscopy for Better Electrochemical Measurements. *Anal. Chem*, 455-461.